Models for field-effect sensors

Clemens Heitzinger

Department of Mathematics & Wolfgang Pauli Institute,
University of Vienna

KTWS3: *Flows and networks in complex media*
April 30, 2009 at IPAM, UCLA

universität wien

Overview

Introduction to field-effect biosensors (BioFETs)

- Short review of experiments

Modeling issues

- Physics-based modeling for the rational design of biosensors
- Development of new algorithms necessary

Modeling and simulation

- Multi-scale modeling and homogenization
- Monte-Carlo simulations
- Stochastics
- Predictive simulations of a proposed new, improved sensor

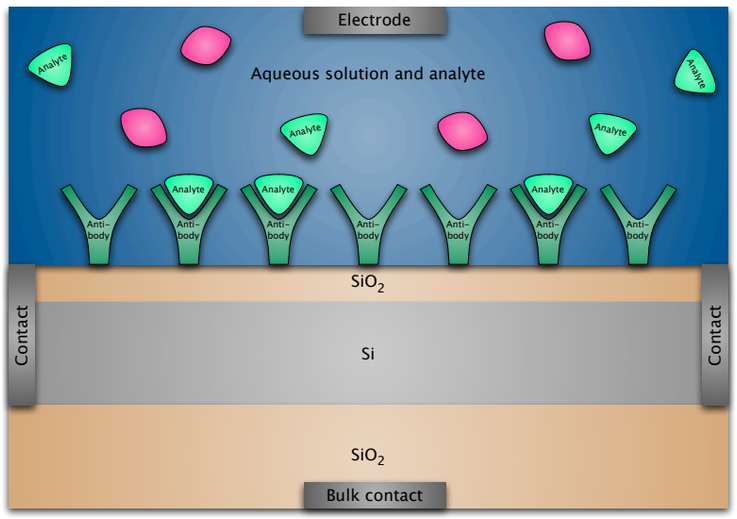

universität wien

BioFETs are field-effect biosensors with semiconducting transducers

Biologically sensitive field-effect transistors (BioFETs) consists of three parts:

- **Receptor**: molecular recognition by functionalized surface.
- **Transducer**: performs the measurement.
  For example Si nanoplates or Si nanowires.
- **Signal processing**.

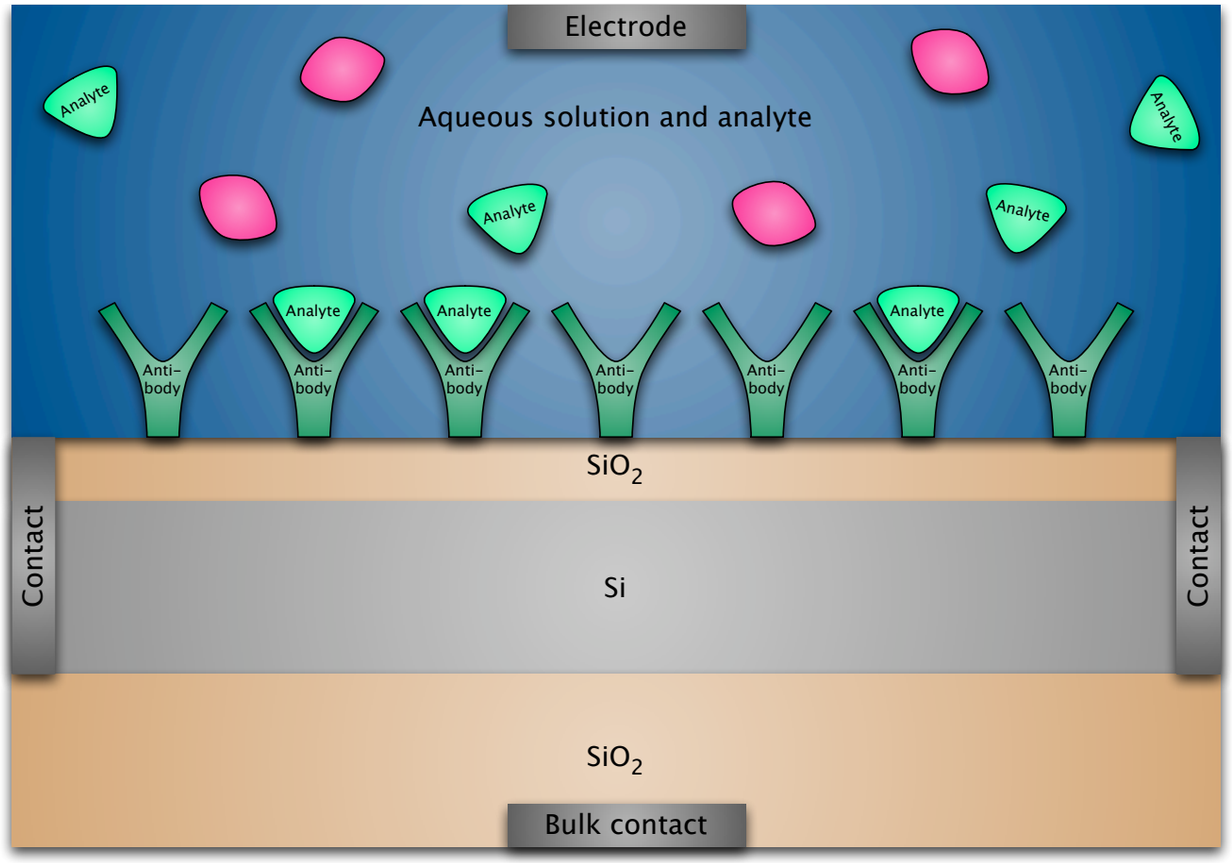

universität wien

A biosensor chip

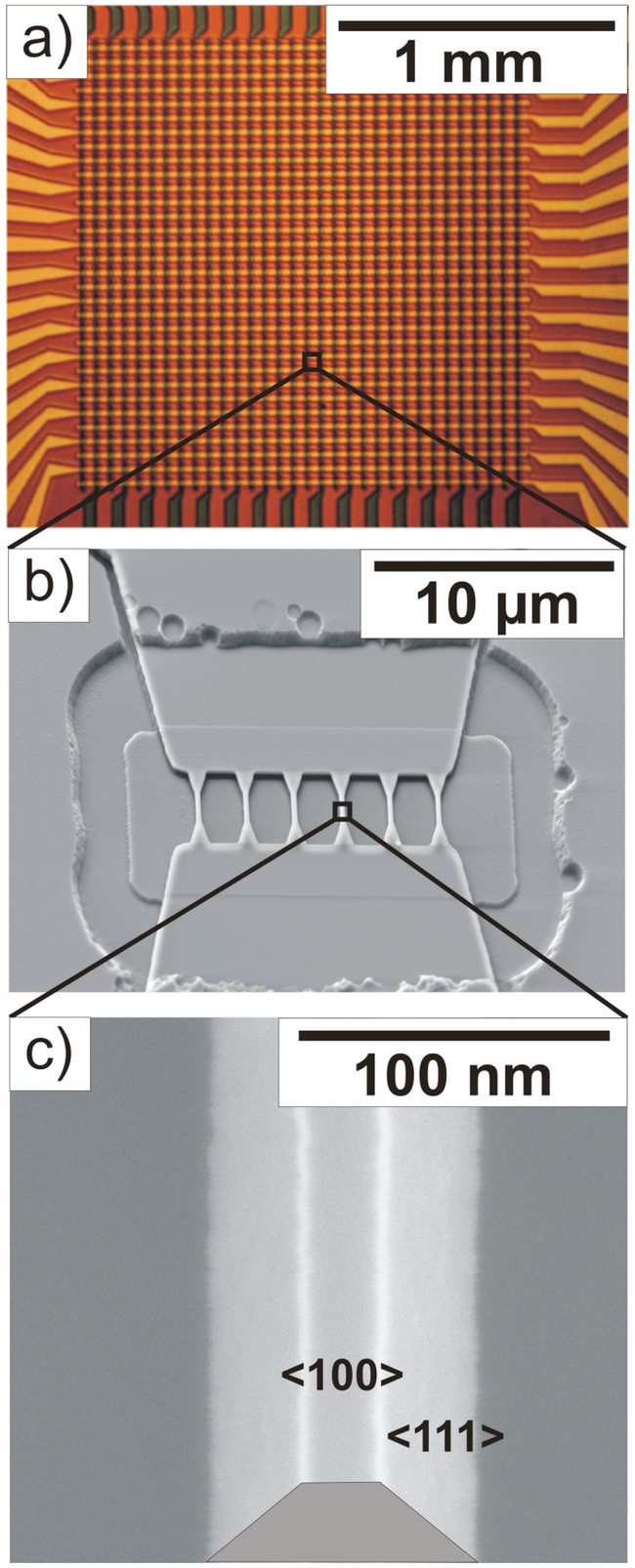

Length scale 1mm:

(a) shows the array of 32 x 32 sensors on the chip.

Length scale 10µm:

(b) shows a single sensor element.
It consists of 6 nanowires.

Length scale 100nm:

(c) shows a single silicon nanowire with a trapezoidal cross section.

Sven Ingebrandt (Fachhochschule Kaiserslautern), Andreas Offenhäusser (Forschungszentrum Jülich), 2008.

universität wien

What are the advantages of BioFETs compared to current technology?

Current technology uses fluorescent or radioactive markers.

The main advantage of field-effect devices is direct, **label-free operation** (no markers are necessary).

Additional advantages are:

- Real-time & continuous sensing.
- No markers change the behavior of the analyte.
- The analyte can be re-used in subsequent experimental steps.
- Read-out circuitry & amplification can be integrated on the chip, which will be important for point-of-care applications.

universität wien

The BioFET concept is a general one with many applications

There are numerous applications depending on how the surface was functionalized:

- Screening for dozens of tumor markers simultaneously (relative change is important).
- Detection of SNPs:
  inherited diseases (like cystic fibrosis, which is one of the most common ones), cancer risk, etc.
- Detection of epigenetic modifications.
- Point-of-care applications
  (NIH's 3 Ps: predictive, personalized, & preemptive medicine).
- DNA sequencing.

universität wien

Silicon-nanowire DNA sensor

Silicon nanowires were grown in the vapor-liquid-solid growth mode.

Note the conductance change in (D) of about 15% to 20%.

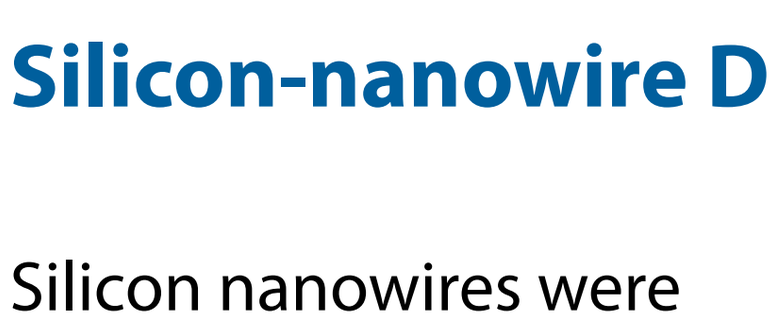

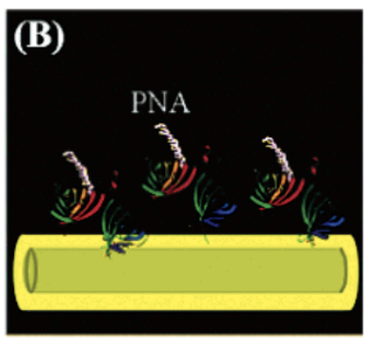

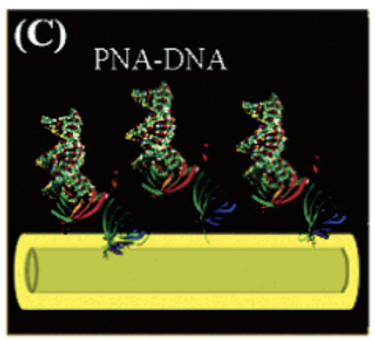

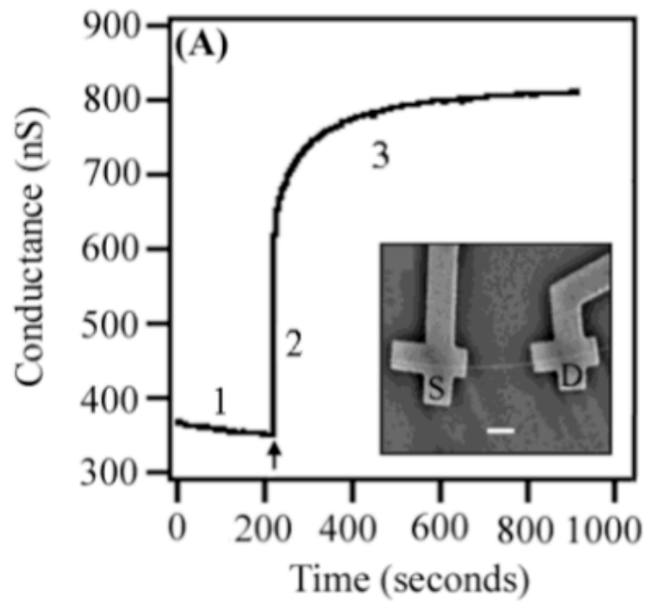

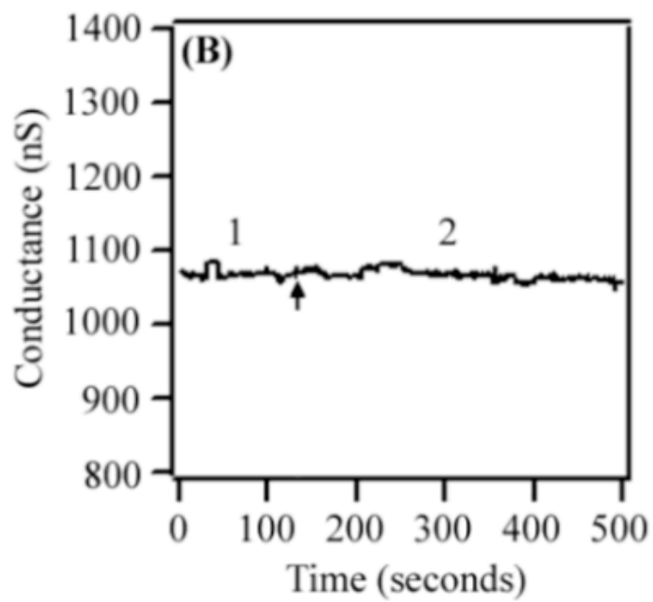

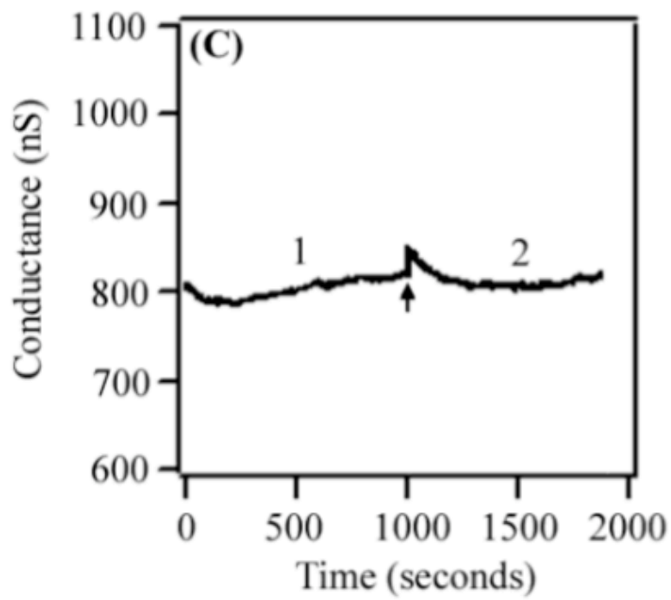

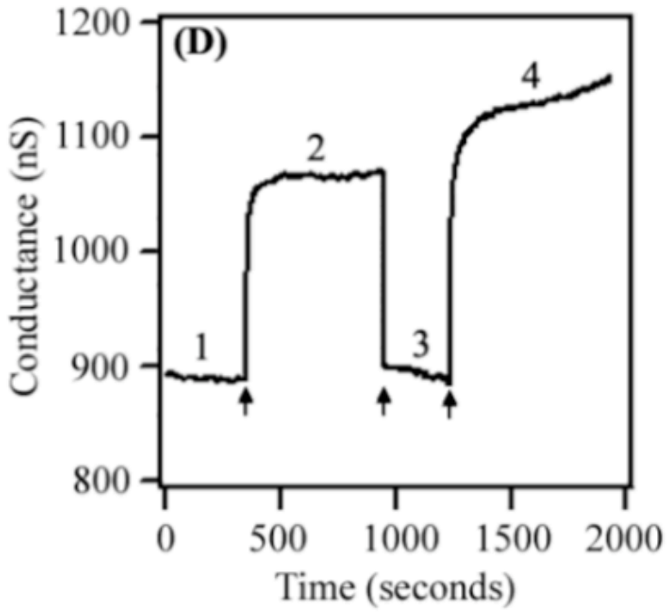

(From: Hahm, Lieber, Nano Lett. **4** 2004)

universität wien

Detection of tumor markers using Si nanowires

Arrays of silicon-nanowire ImmunoFETs enable highly sensitive (0.9pg/ml) detection of cancer markers:

- PSA (prostate specific antigen): increased levels indicate localized or metastatic prostate cancer.
- CEA (carcinoembryonic antigen): a glycoprotein involved in cell adhesion; increased levels indicate colorectal cancer.
- Mucin-1.

(1) 0.9ng/ml PSA
(2) 1.4pg/ml PSA
(3) 0.2ng/ml CEA
(4) 2.0pg/ml CEA
(5) 0.5ng/ml mucin-1
(6) 5.0pg/ml mucin-1

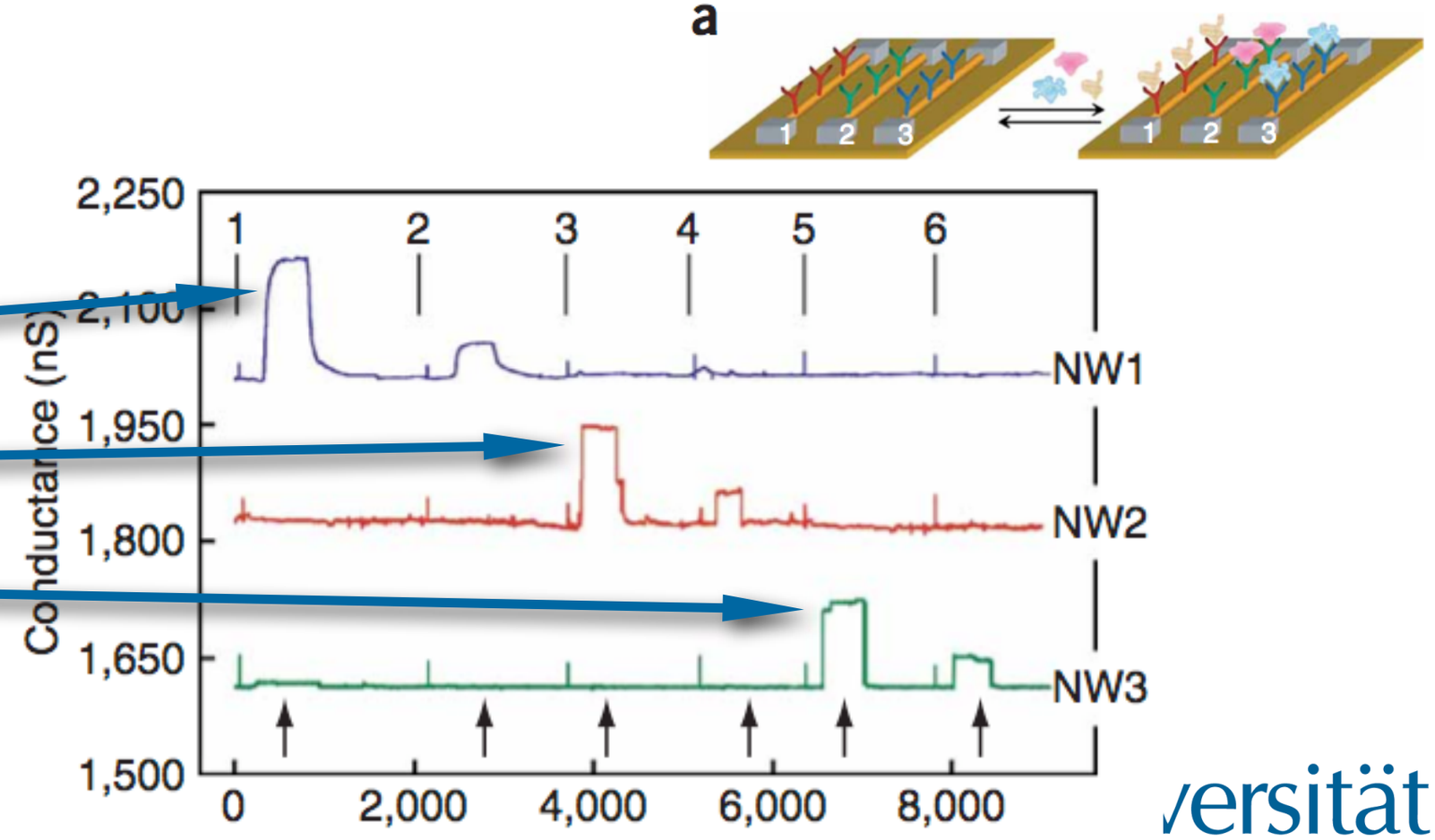

(From: Zheng et al., nature biotechnology **23** 2005)

Universität Wien

DNA detection using Si nanowires in arrays

PNA (peptide nucleic acid) probes were used to detect ssDNA.

The sensors discriminate satisfactorily against mismatched target DNA.

Detection limit of 10 fM.

Response time is not very good.

Huge resistance change (!).

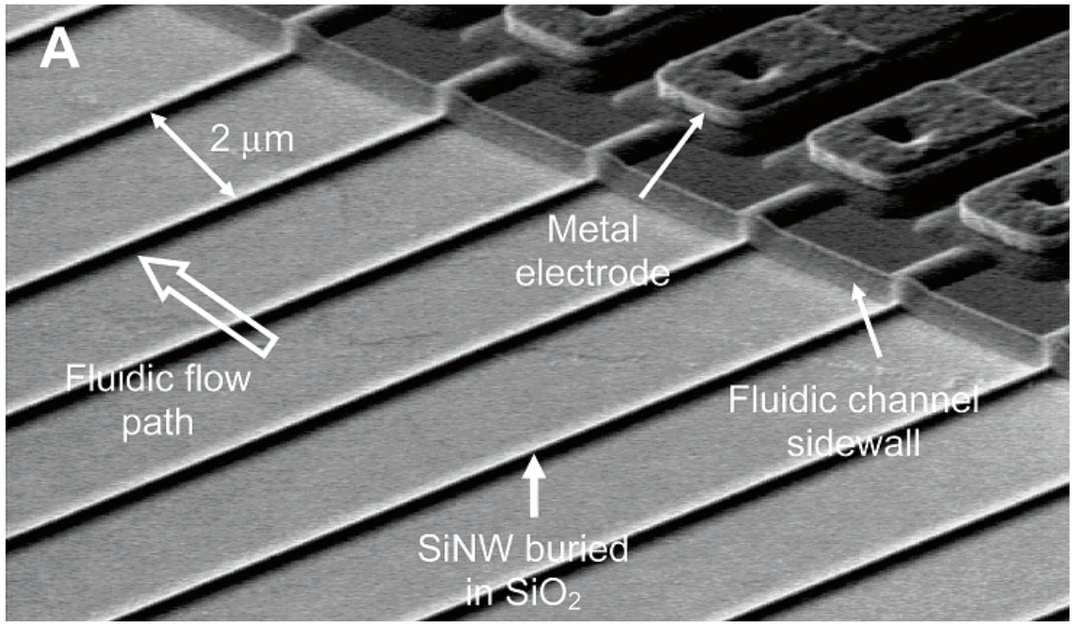

(From: Gao et al., Analytical Chemistry **79** 2007)

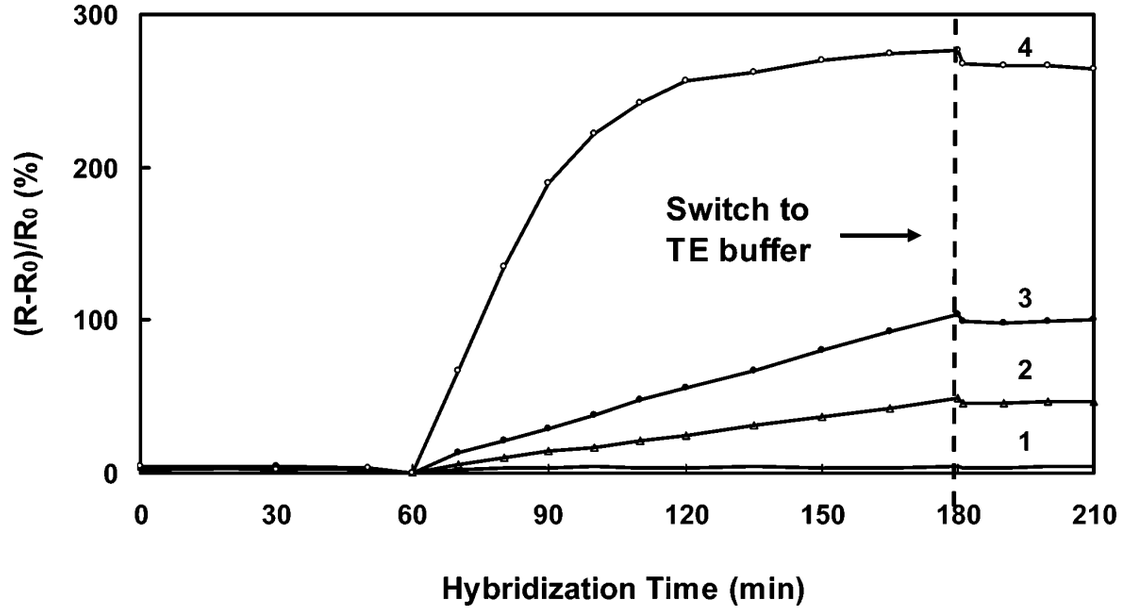

Figure 5. The dependence of resistance change of the SiNW array biosensor on hybridization time in (1) 1.0 nM control, (2) 25 fM, (3) 100 fM and (4) 1.0 nM target DNA in TE buffer.

universität wien

Antigen detection using Si nanowires

Traditionally, nanowires are made in the vapor-liquid-solid growth mode and assembled.

However, assembly is very time-consuming.

Here Si nanowires were fabricated in a top-down **CMOS-compatible** approach.

- Si nanowires: 40nm thick and 50nm to 150nm wide.
- Surface receptors: antibodies.
- 10fM concentrations of treptavidin were detected.

Special microfluidic channel and pump for fast response time.

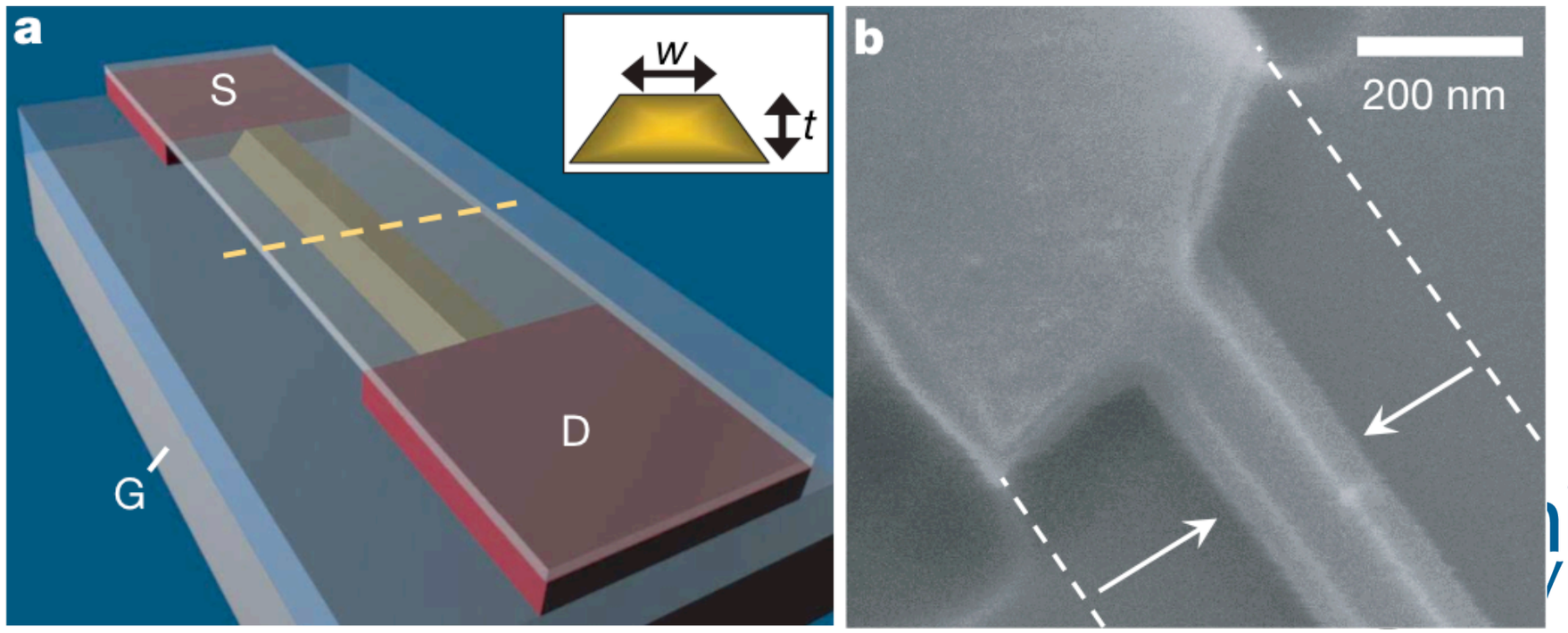

(From: Stern et al., nature **445** 2007)

niversität
ien

The Debye length and field-effect sensors

The Debye length is the mean distance where the effect of a charge can still be noticed despite screening.

It is ca. 1nm at physiologically relevant concentrations (serum: ca. 160mM). Therefore it was believed for a long time that field-effect sensors would not work.

Smaller ionic concentration reduces the Debye length, but a certain ionic concentration is necessary for DNA hybridization.

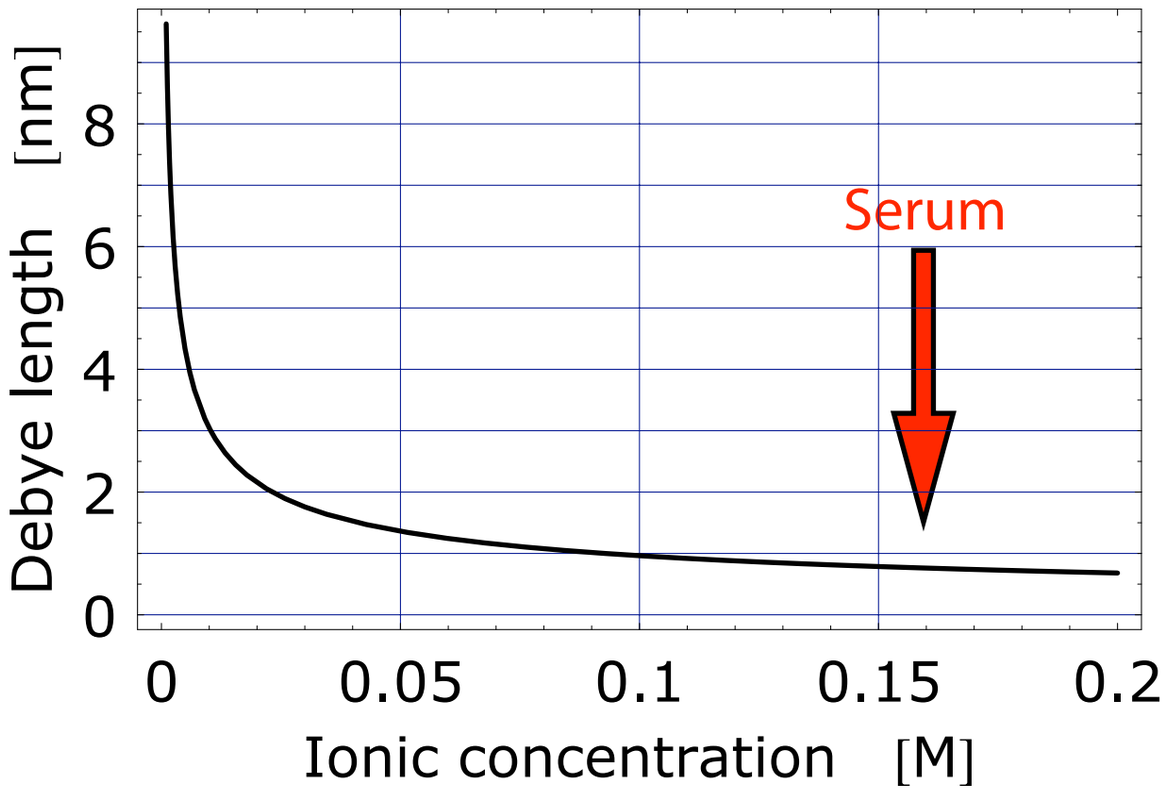

universität wien

The different types of charges in the system

Electrostatics are governed by the **Poisson equation**:

$$-\partial_x\big(\epsilon(x)\partial_x V(x,\mathbf{y})\big) - \nabla_{\mathbf{y}}\cdot\big(\epsilon(x)\nabla_{\mathbf{y}} V(x,\mathbf{y})\big) = n_T\big(V(x,\mathbf{y}),x,\mathbf{y}\big) + n_E(x,\mathbf{y})$$

Self-consistent modeling of:

- **Biophysical** part:
  - Continuum model:
    Poisson–Boltzmann equation
  - Atomistic model:
    (Metropolis) Monte Carlo simulations
- **Nano-electronic** part:
  - Classical models:
    - drift-diffusion (with QM corrections)
    - Boltzmann equation (with QM corr.)
  - Quantum-mechanical models:
    - Effective quantum potentials
    - Non-equilibrium Green functions
    - Wigner functions, etc.

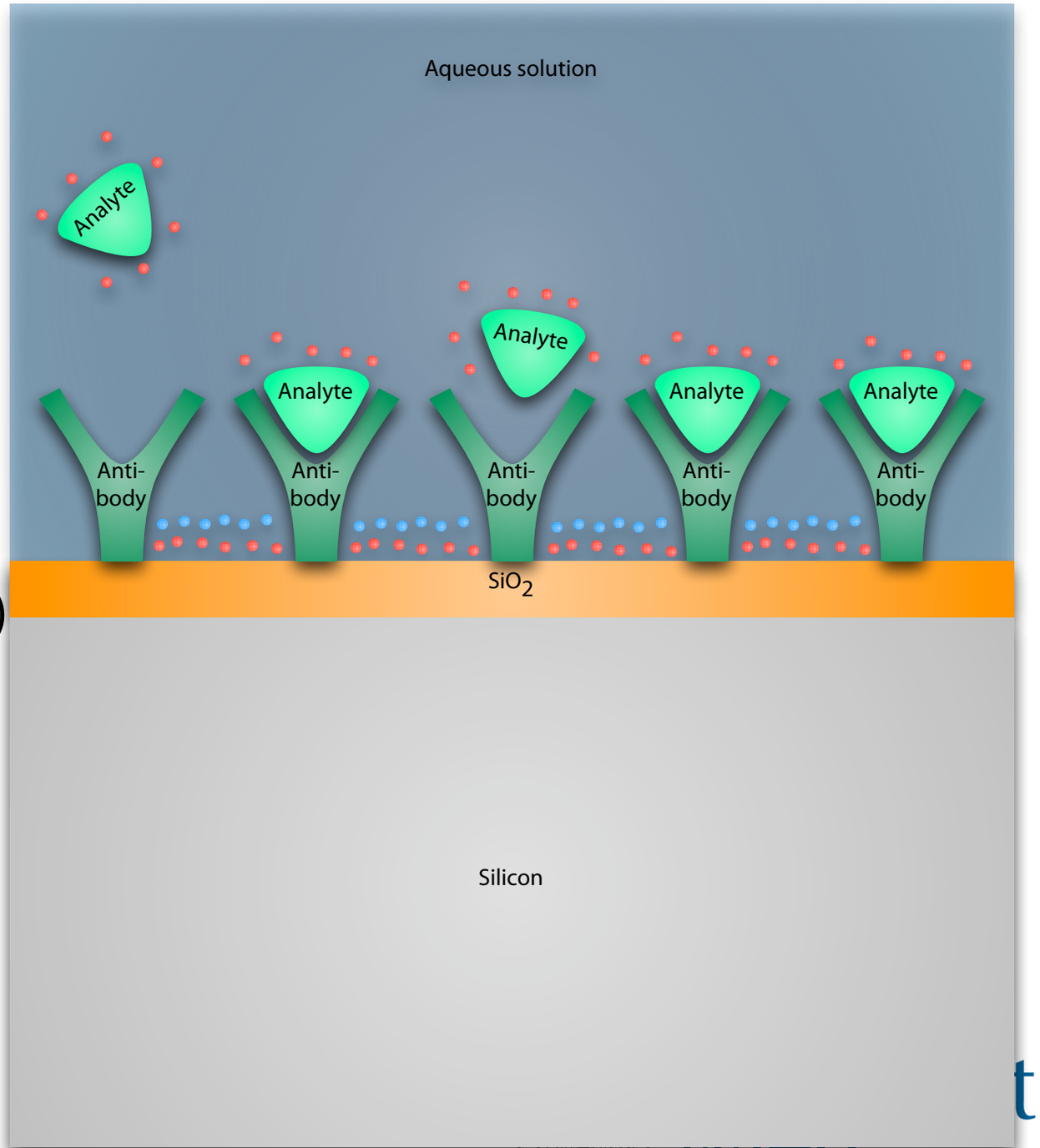

The multi-scale problem

We are dealing with two different length scales:

- DNA diameter: 2nm; hence the electrostatic potential around the biomolecules varies on the Angstrom scale;
- length of the sensor area: a few micrometer.

Simple idea: just use a semiconductor device simulator with a very fine grid. **Not possible!**

$$n(r,\phi,z) := \begin{cases} \chi(r,\phi,z) & \text{for } r > r_1, \\ n_<(r,\phi,z) & \text{for } r < r_1 \end{cases}$$

fast-varying

doping

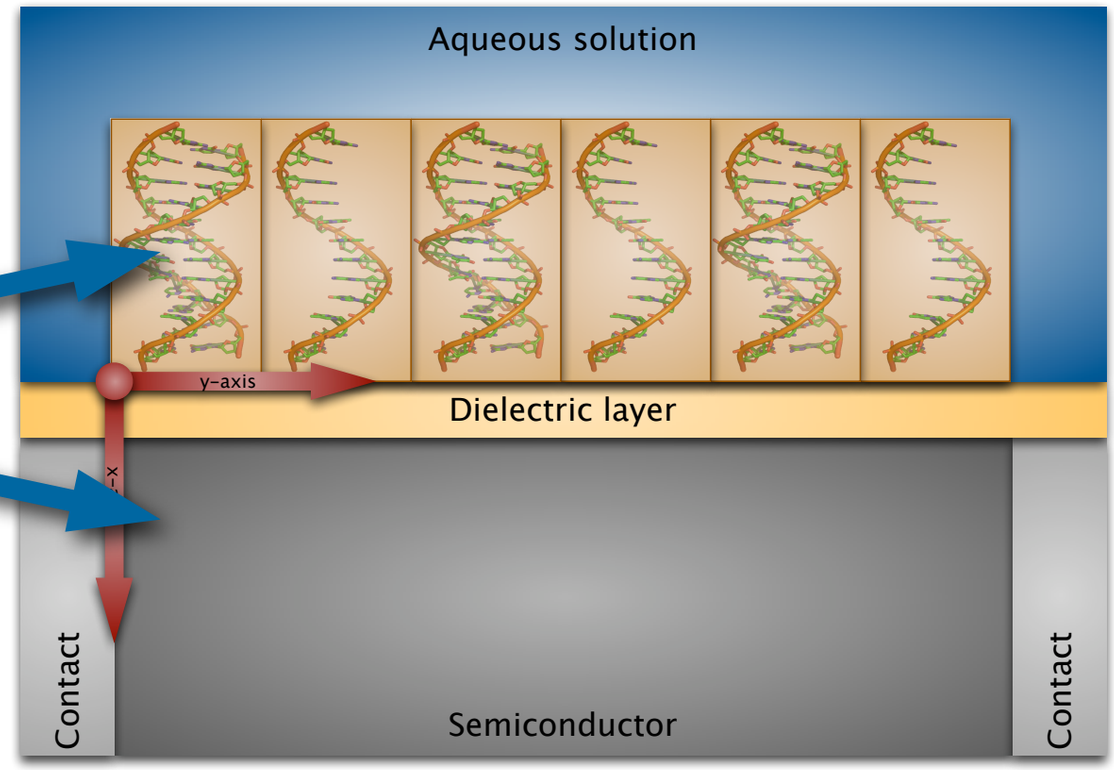

universität wien

Theorem for the limiting problem λ→0

Theorem (CH, Ringhofer 2008). Let $R := [0, r_2]$, $L := [0, 2\pi) \times [0, L_z]$, and $\Omega := R \times L \subset \mathbb{R}^3$. Let $r_1 \in (0, r_2)$, let $\epsilon : R \to \mathbb{R}^+$ with

$$\epsilon(r) = \begin{cases} \epsilon_< \in \mathbb{R} & \text{for } r < r_1, \\ \epsilon_> \in \mathbb{R} & \text{for } r > r_1, \end{cases}$$

and let $n \in L^2(\Omega)$ with

$$n(r, \mathbf{y}) := \begin{cases} n_<(r, \mathbf{y}) \in L^2\big([0, r_1) \times L\big) & \text{for } r < r_1, \\ \chi(r, \mathbf{y}) \in L^2\big((r_1, r_2) \times L\big) & \text{for } r > r_1, \end{cases}$$

where $n_<$ is bounded and χ is a boundary layer function such that $C(\mathbf{y})$ and $D_r(\mathbf{y})$ exist.

The limiting problem for $\lambda \to 0$ of the boundary value problem

$$-\nabla \cdot \big(\epsilon(r)\nabla\big) V(r, \mathbf{y}) = n(r, \mathbf{y}), \tag{1a}$$
$$V(r_1-, \mathbf{y}) = V(r_1+, \mathbf{y}), \tag{1b}$$
$$\epsilon_< \partial_r V(r_1-, \mathbf{y}) = \epsilon_> \partial_r V(r_1+, \mathbf{y}) \tag{1c}$$

with $(r, \mathbf{y}) \in \Omega$ is the boundary value problem

$$-\epsilon_< \left(\frac{1}{r}\partial_r(r\partial_r) + \frac{1}{r^2}\partial_{\phi\phi} + \partial_{zz}\right) V_h(r, \mathbf{y}) = n_<(r, \mathbf{y}) \quad \text{for } r < r_1, \tag{2a}$$
$$-\epsilon_> \left(\frac{1}{r}\partial_r(r\partial_r) + \frac{1}{r^2}\partial_{\phi\phi} + \partial_{zz}\right) V_h(r, \mathbf{y}) = 0 \quad \text{for } r > r_1 \tag{2b}$$

with the interface conditions

$$V_h(r_1+, \mathbf{y}) - V_h(r_1-, \mathbf{y}) = \frac{D_r(\mathbf{y})}{\epsilon_>}, \tag{3a}$$
$$\epsilon_> \partial_r V_h(r_1+, \mathbf{y}) - \epsilon_< \partial_r V_h(r_1-, \mathbf{y}) = -C(\mathbf{y}). \tag{3b}$$

λ (λ→0) is the ratio of the size of a cell to the whole domain.

← The original problem becomes

← the homogenized problem

← with certain interface conditions.

universität wien

Outline of the proof

λ is the ratio of the size of one cell to the whole domain.

Homogenization procedure:

- We split the boundary into cells.
- We remove the jump in the permittivity at the interface by stretching the r-coordinate.
- We use the weak formulation.
- The limit $\lambda \to 0$ is calculated using the multi-scale ansatz and Taylor expansions.
- We compare the coefficients of the test function and its derivative between the weak formulation and the ansatz for the strong formulation.
- This yields the interface (jump) conditions and C and D.

We also proved generalizations to arbitrary geometries.

universität wien

Theorem for the limiting problem λ→0: what determines the interface conditions?

Definition 1 (Macroscopic surface charge density)**.** *Let χ be a boundary layer function. Then the macroscopic surface charge density $C(\mathbf{y})$ is defined as*

$$C(\mathbf{y}) := \lim_{\lambda\to 0} \frac{\lambda}{2\pi r_1 L_z} \int_L \int_{r_1}^{r_2} \chi(\rho, \boldsymbol{\eta}, \mathbf{y}) \big(r_1 + \lambda(\rho - r_1)\big) \mathrm{d}\rho \mathrm{d}\boldsymbol{\eta}. \tag{1}$$

Definition 2 (Macroscopic dipole moment density)**.** *Let χ be a boundary layer function. The macroscopic dipole moment density $D(\mathbf{y})$ is defined as*

$$D(\mathbf{y}) := \begin{pmatrix} D_r(\mathbf{y}) \\ D_{\mathbf{y}}(\mathbf{y}) \end{pmatrix} := \lim_{\lambda\to 0} \frac{\lambda^2}{2\pi r_1 L_z} \int_L \int_{r_1}^{r_2} \begin{pmatrix} \rho - r_1 \\ \boldsymbol{\eta} \end{pmatrix} \chi(\rho, \boldsymbol{\eta}, \mathbf{y}) \big(r_1 + \lambda(\rho - r_1)\big) \mathrm{d}\rho \mathrm{d}\boldsymbol{\eta}. \tag{2}$$

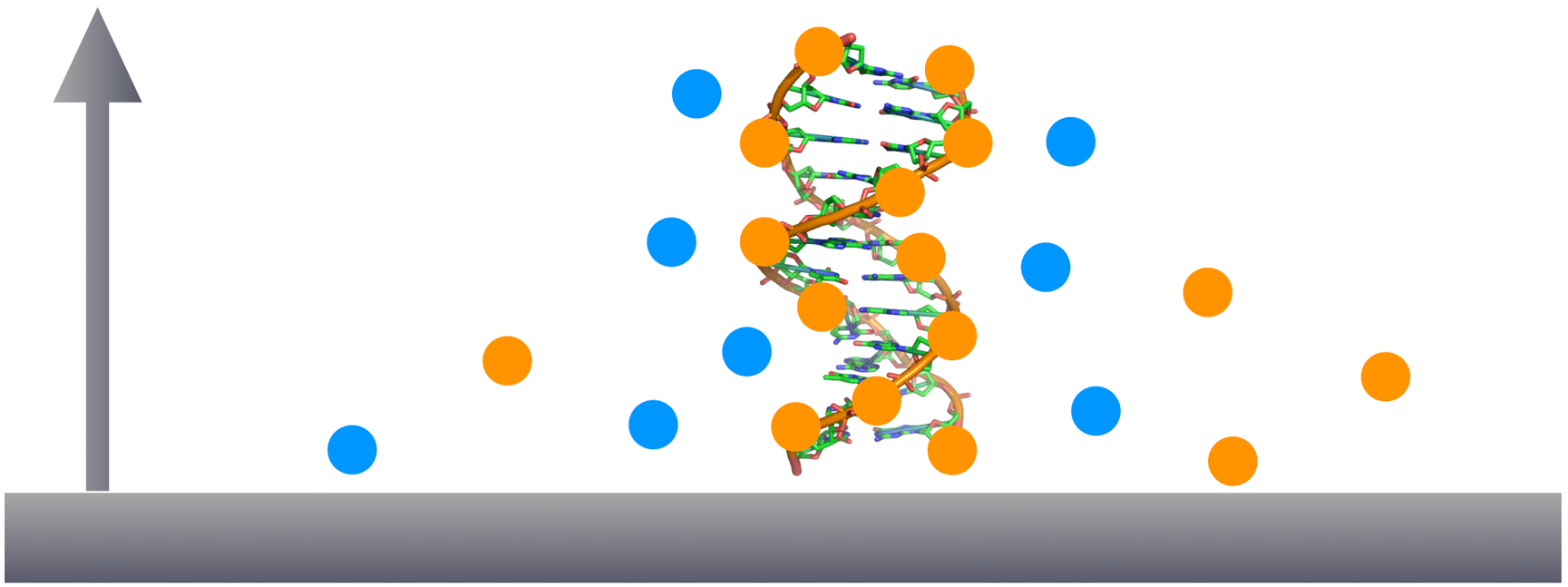

universität wien

How can we calculate the charge densities and dipole moments of the boundary layer?

We construct B-DNA strands from the coordinates of single nucleotides.

Arbitrary sequences, linker lengths, and orientations with respect to the surface are possible.

We use a GROMACS force field to obtain the partial charges of the probe and target molecules (and the locations of the hydrogens).

The same procedure can be used for any biomolecule whose structure is known (seee PDB, for example).

To calculate the electrostatics and charge distributions, we are using two methods:

- solve the Poisson-Boltzmann equation or
- perform Metropolis Monte Carlo calculations.

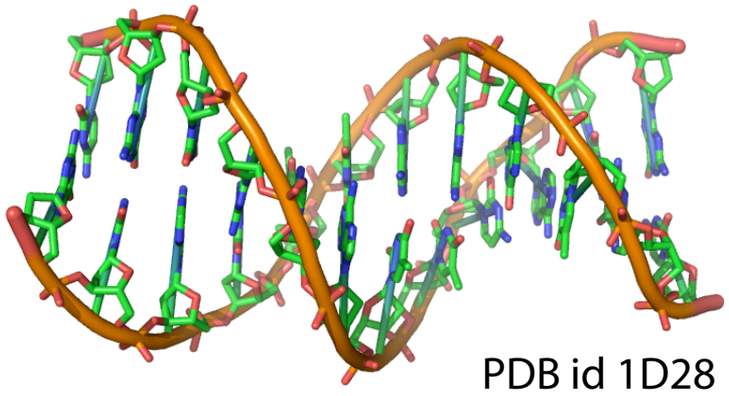

PDB id 1D28

universität wien

1D simulation of nanoplates and different DNA strand lengths

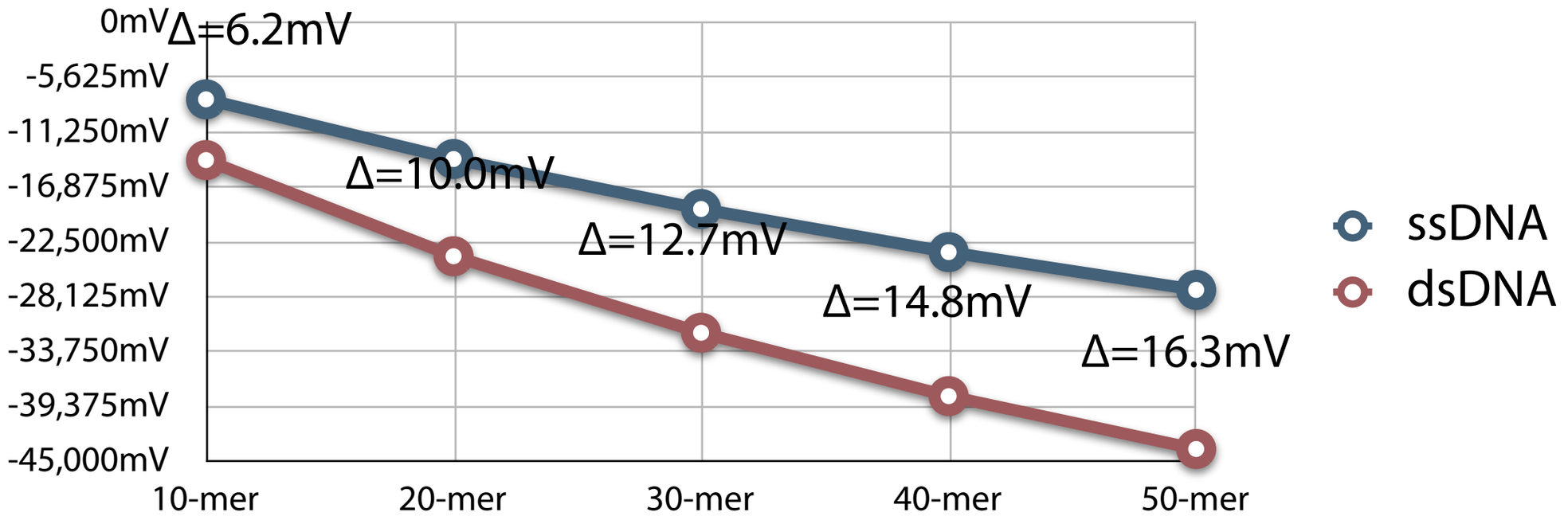

1D simulation of a nanoplate DNA-FET:

- Binding efficiency: 100%;
  oxide thickness: 2nm; Si nanoplate thickness: 30nm.

Experimental data from Fritz et al., PNAS **99** 2002:

- Oxide thickness: 2nm;
  12-mer oligonucleotides;
  surface potential change: about 5mV depending on concentration (i.e., binding efficiency).

universität wien

2D self-consistent simulations using the drift-diffusion model for a silicon-nanowire sensor

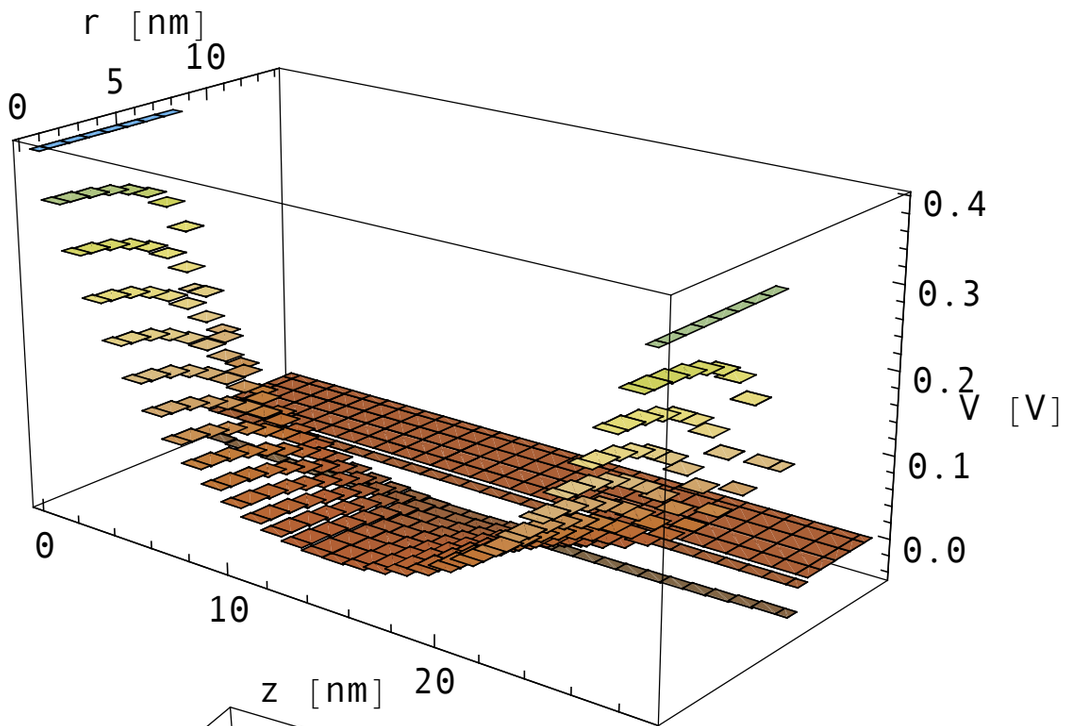

$$J_n = -q\mu_n n\nabla V + qD_n\nabla n$$

$$J_p = -q\mu_p p\nabla V - qD_p\nabla p$$

$$\nabla \cdot J_n = q\partial_t n + qR$$

$$\nabla \cdot J_p = -q\partial_t p - qR$$

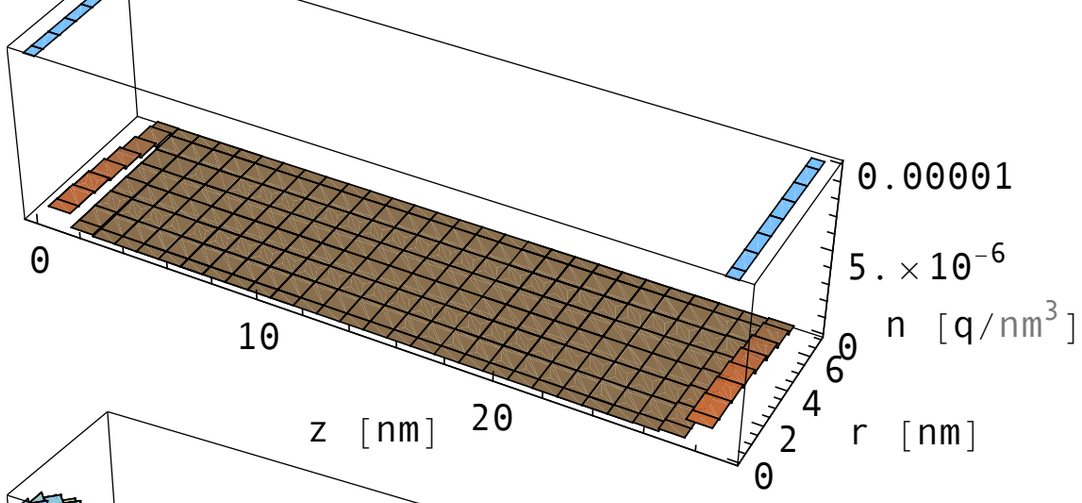

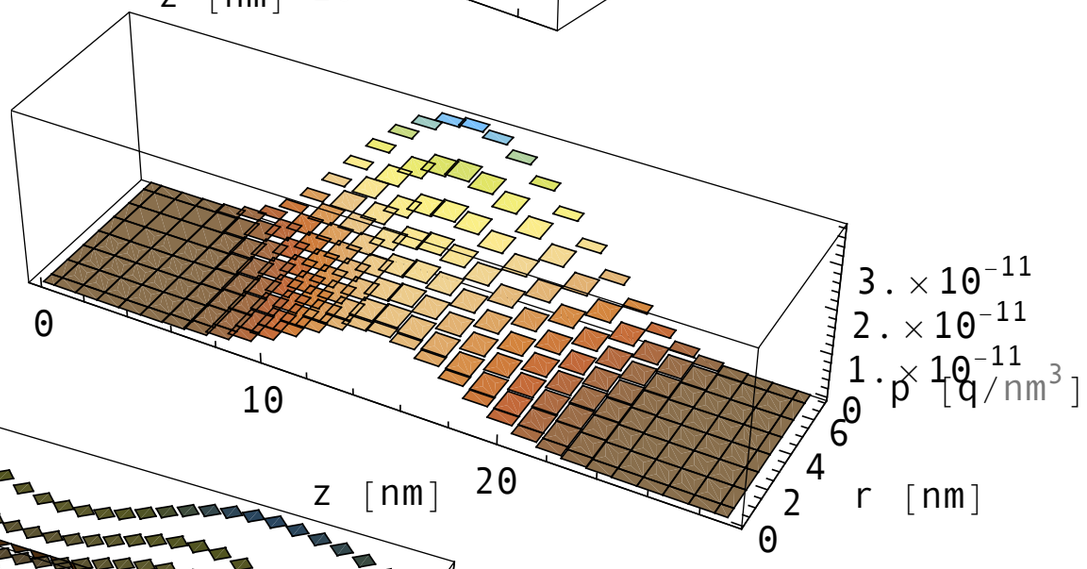

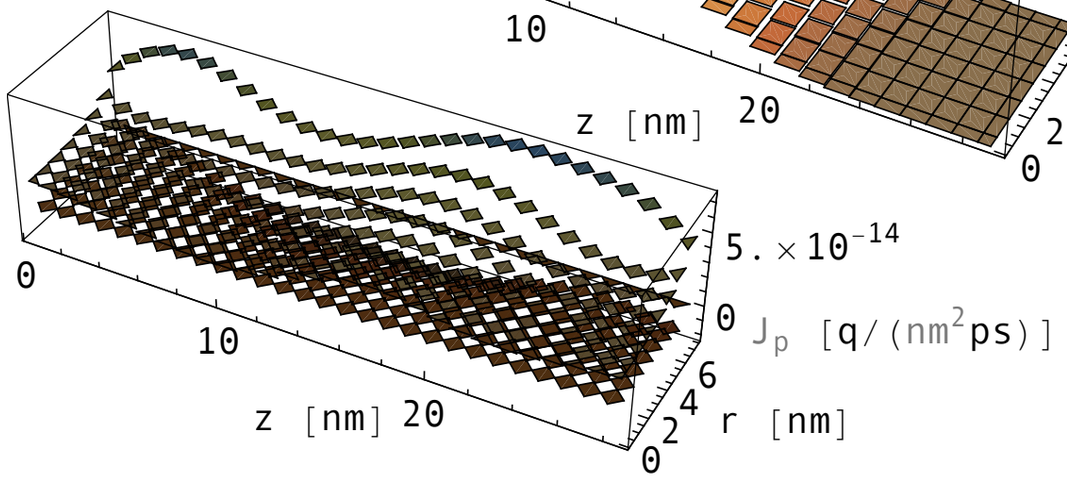

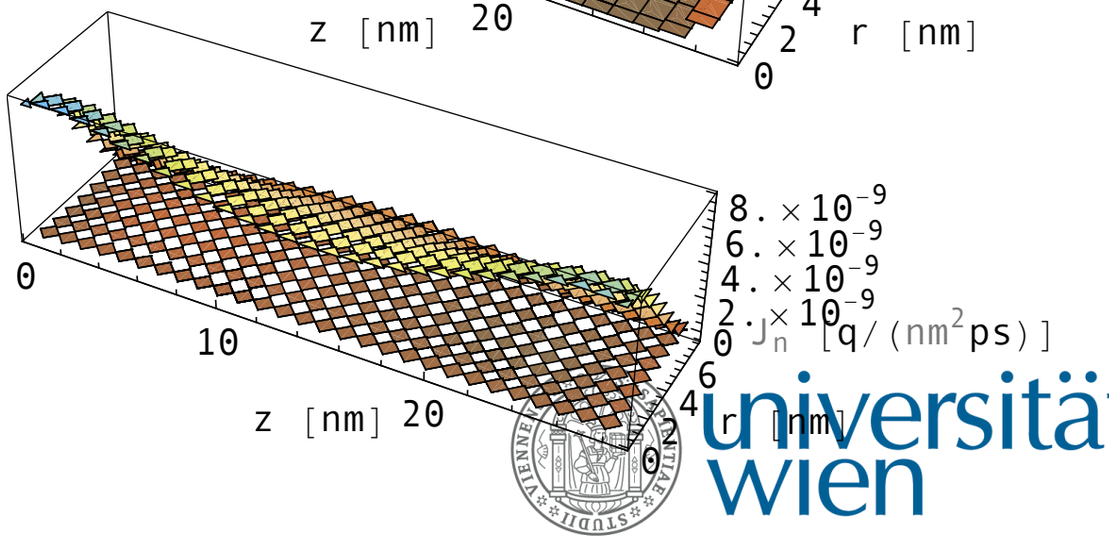

universität wien

Conductance of a silicon-nanowire sensor

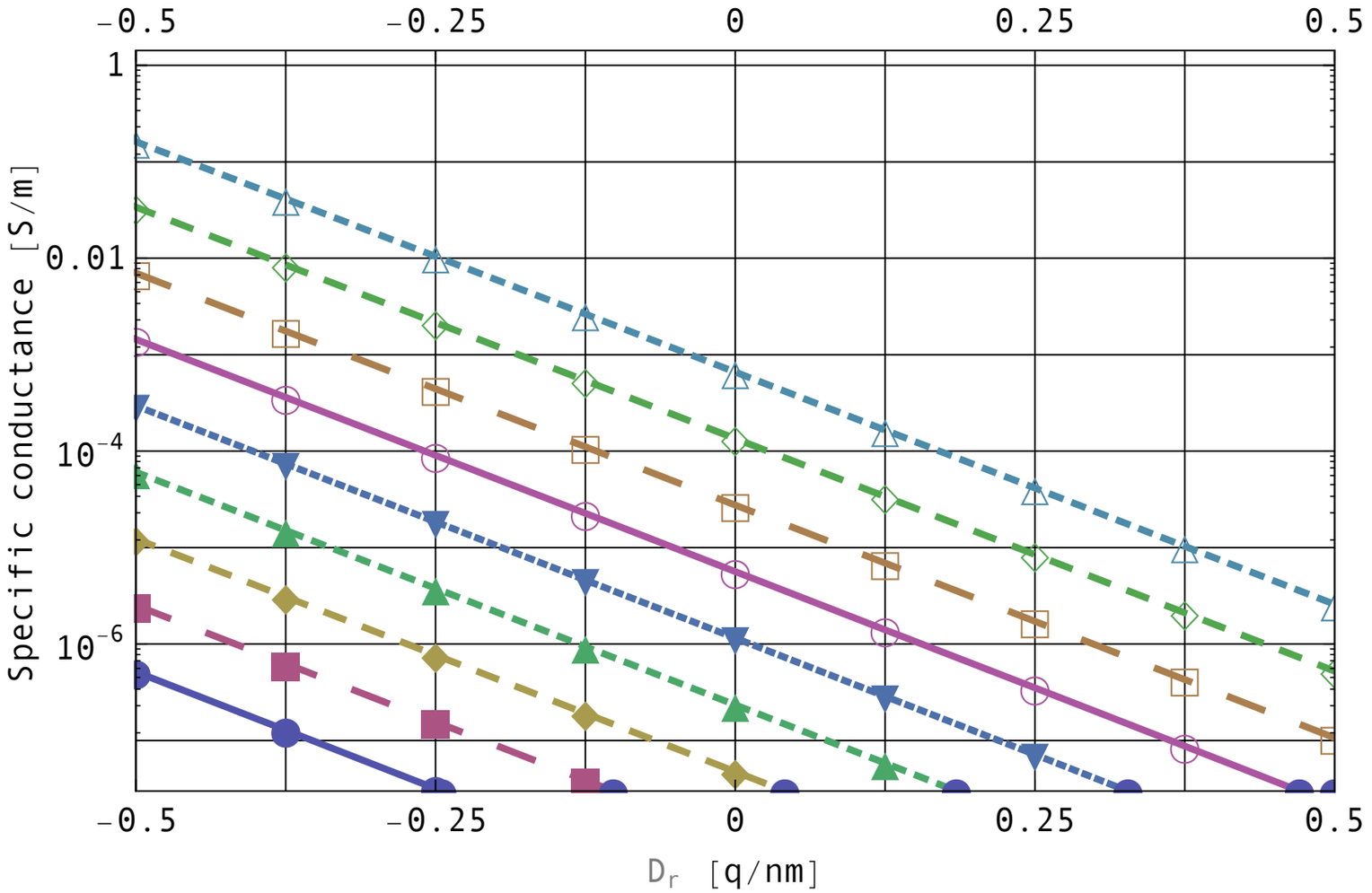

The bottom line (blue, solid line with solid circles) is for C=–0.5q/nm^{-2}.

The top line (light blue, dashed line with hollow triangles) is for C=+0.5q/nm^{-2}.

Step size in C: 0.125q/nm^{-2}.

We use the homogenization theorem for cylindrical geometries.

Here the specific conductance (from the 2D DD model) is shown as a function of the dipole moment density of the biofunctionalized layer.

The liquid contains 10^{-6} mol/L of Na^+Cl^-. The p-doped (10^{16}cm^{-3}) Si nanowire is 100nm long, the silicon core has a radius of 5nm, and the silicon oxide layer has a thickness of 2nm.

universität wien

MC simulations of the surface layer: the electric double layer, PNA, ssDNA, & dsDNA

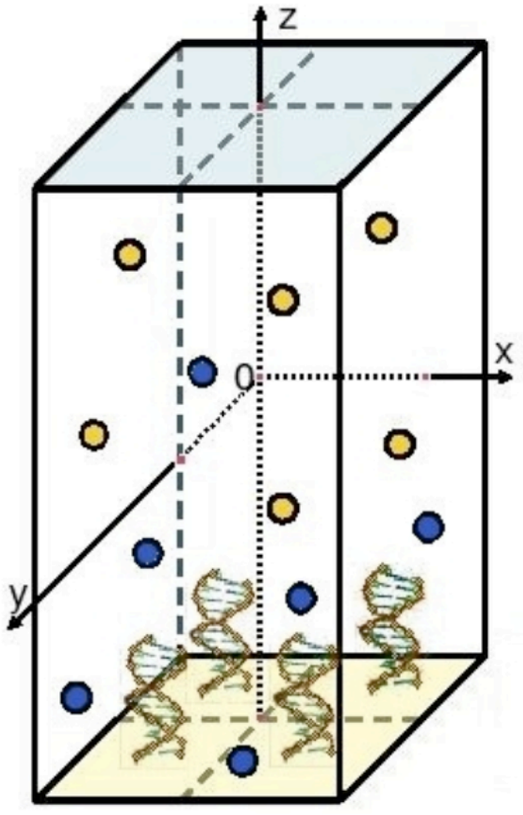

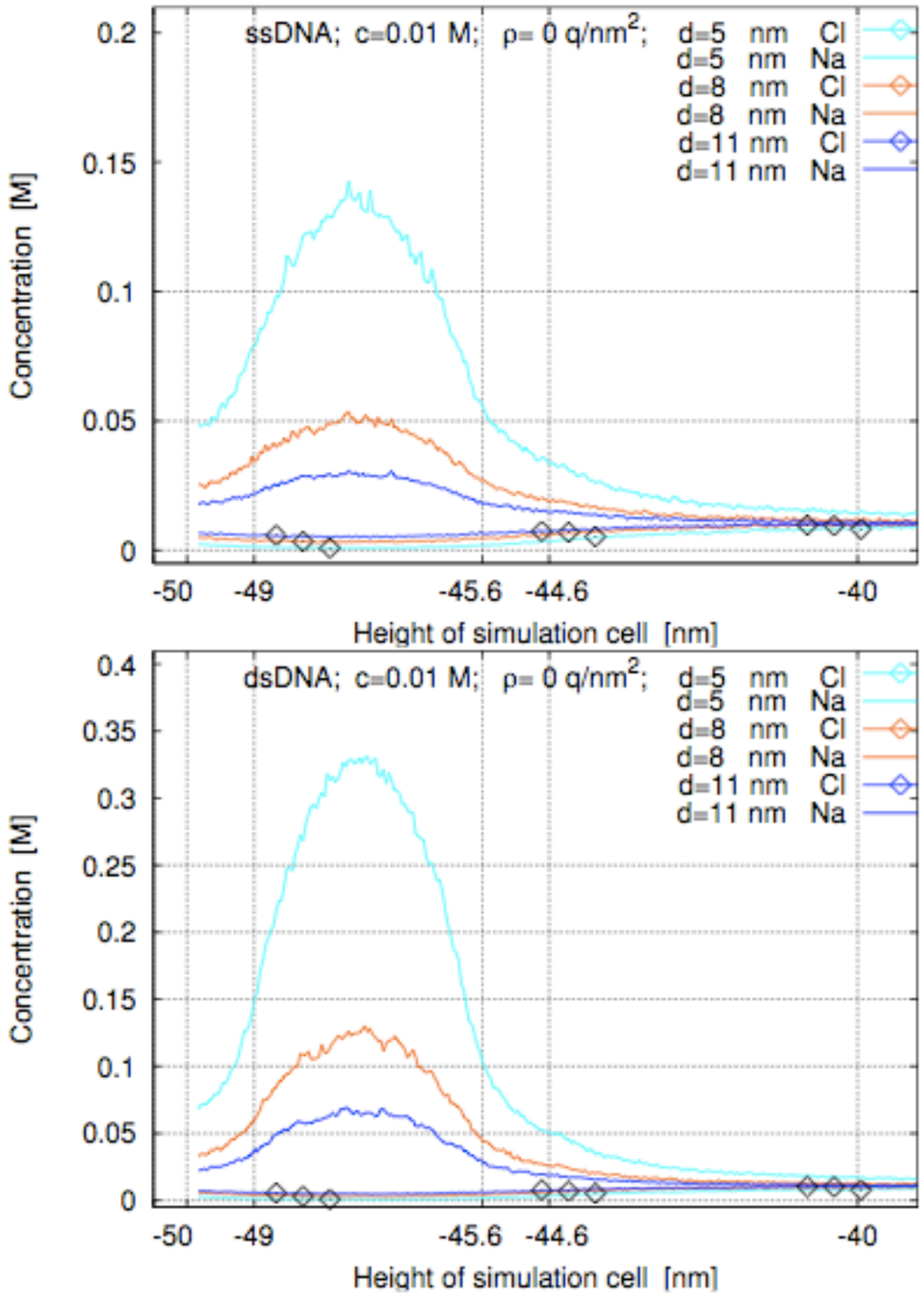

universität wien

MC simulations:
the influence of probe spacing

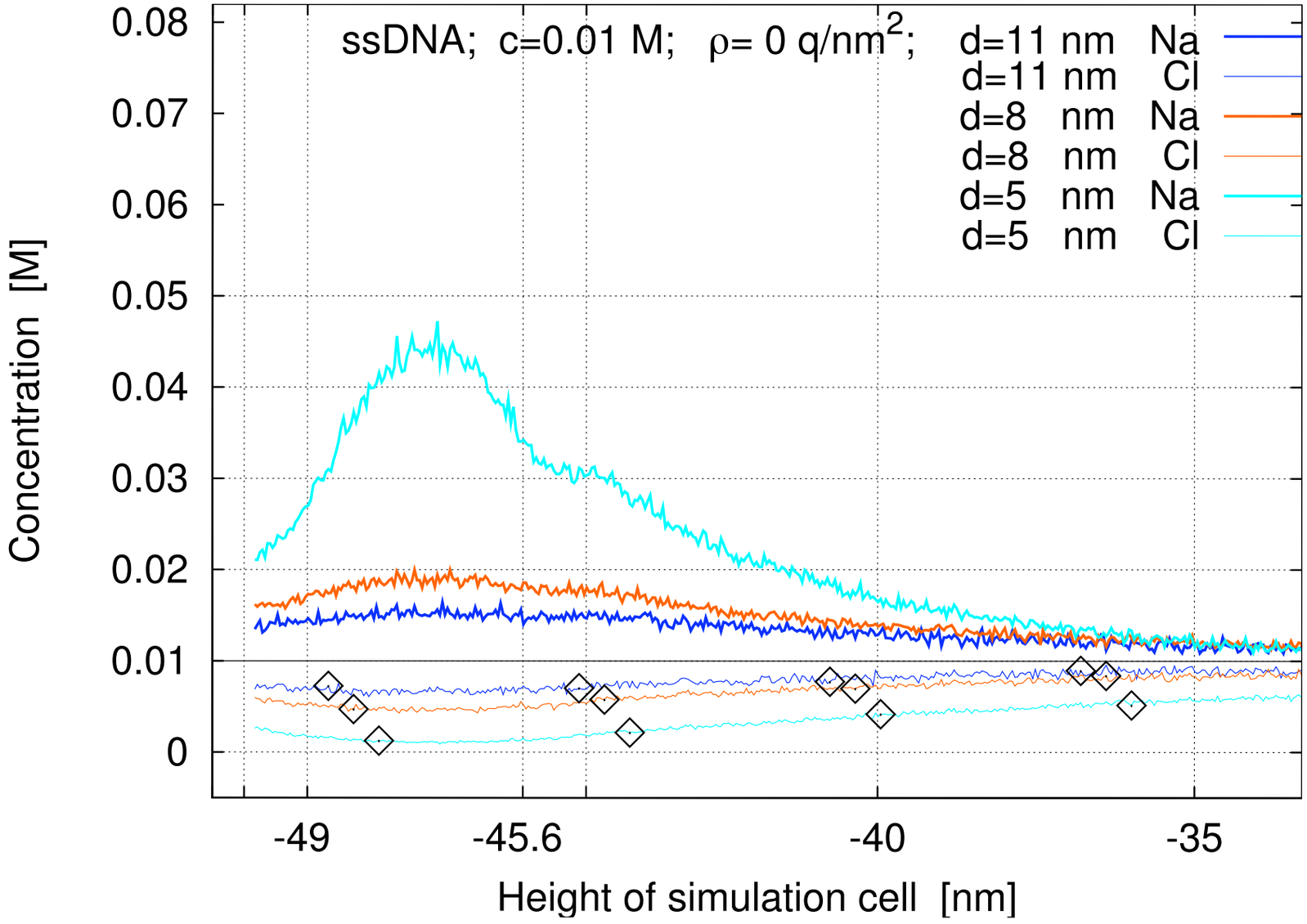

universität wien

MC simulations:
the influence of surface (oxide) charge density

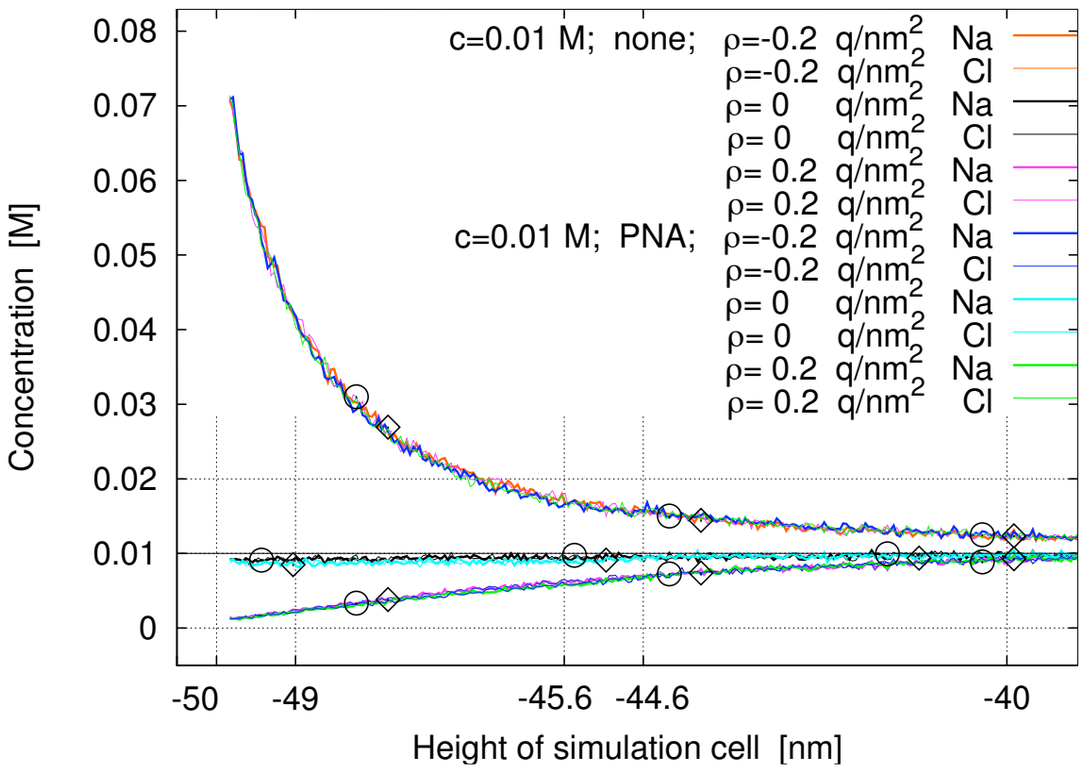

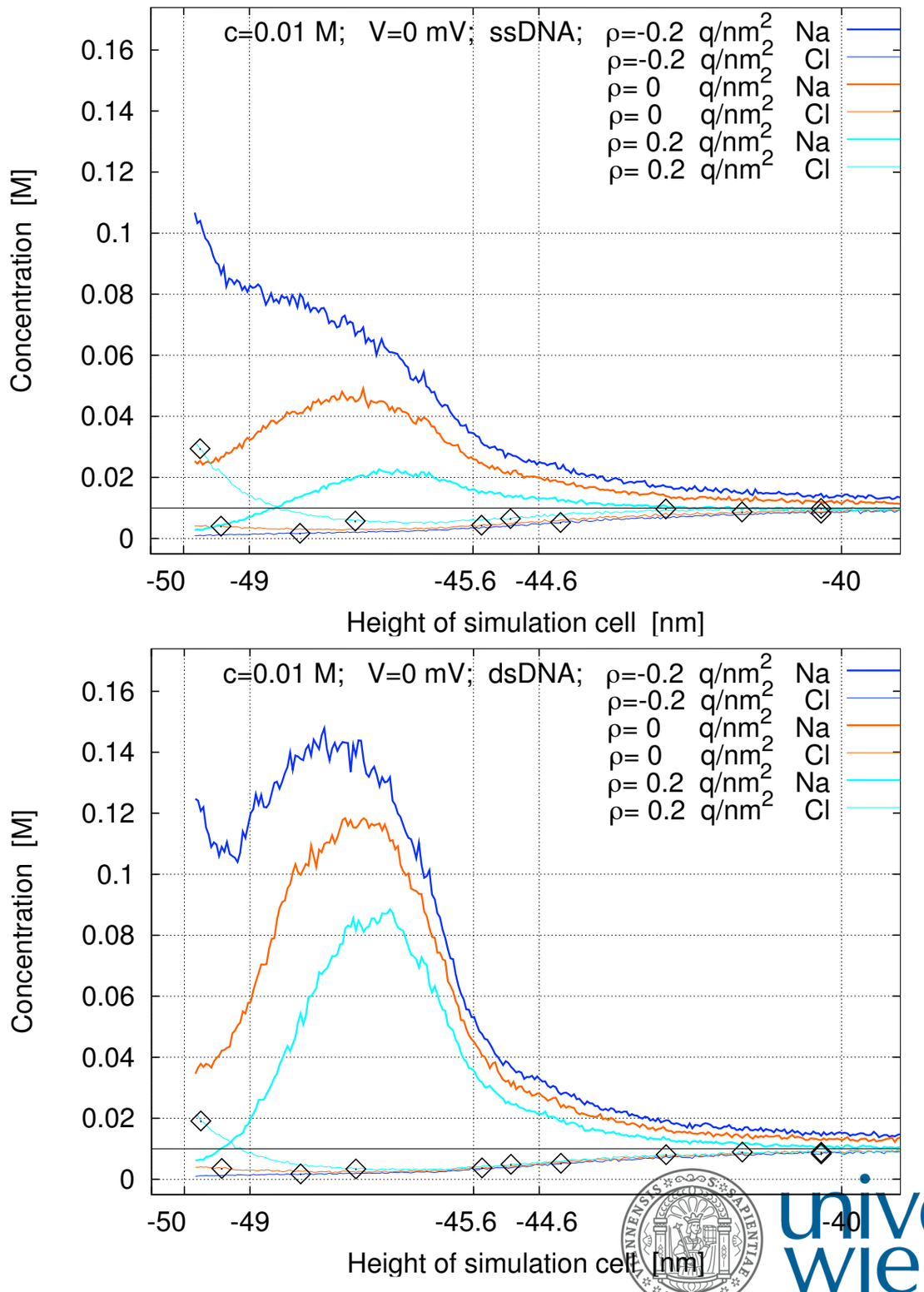

universität wien

MC simulations: the influence of applied voltage

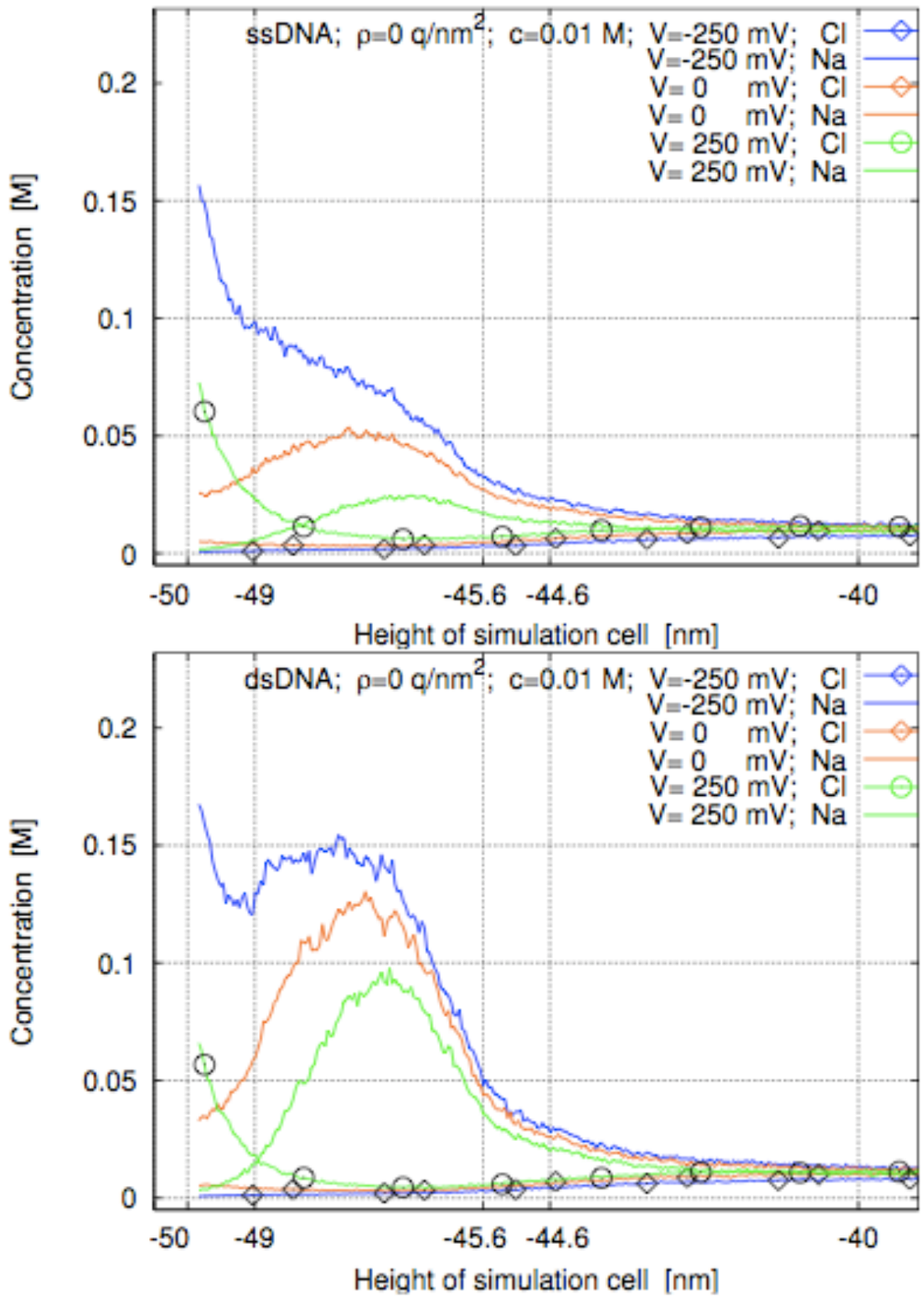

universität wien

MC simulations: three-layer behavior

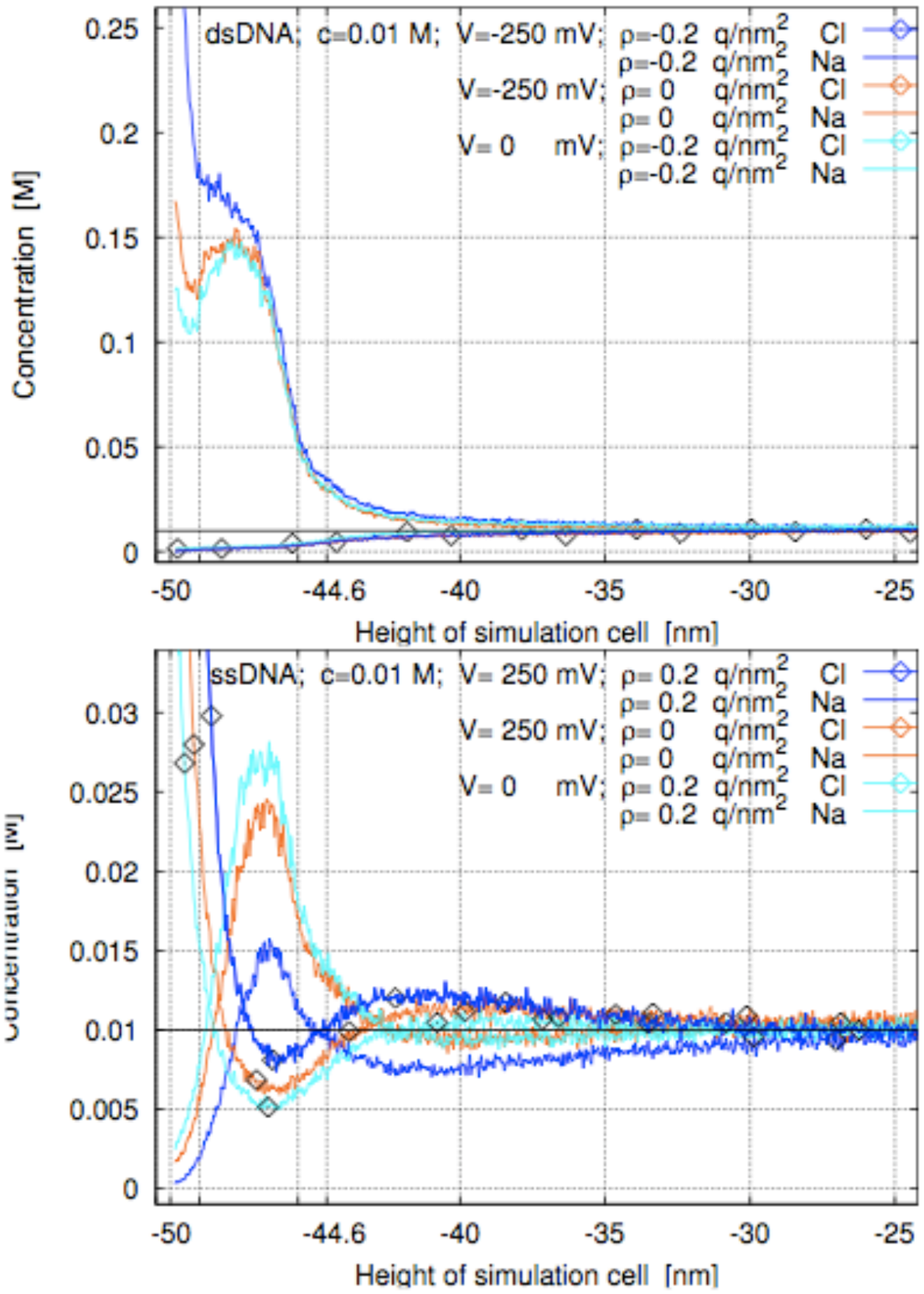

universität wien

Self-consistent loop between microscopic (PB) and macroscopic (DD) simulations

The microscopic model is the Poisson–Boltzmann equation:
surface charge density –0.2q/nm^2, 5nm boxes, 100mM NaCl,
C…solid lines, D…dashed lines,
no molecule…black lines, ssDNA…blue lines, dsDNA…red lines.

The macroscopic model is drift-diffusion for a silicon nanowire.

No fitting parameters!

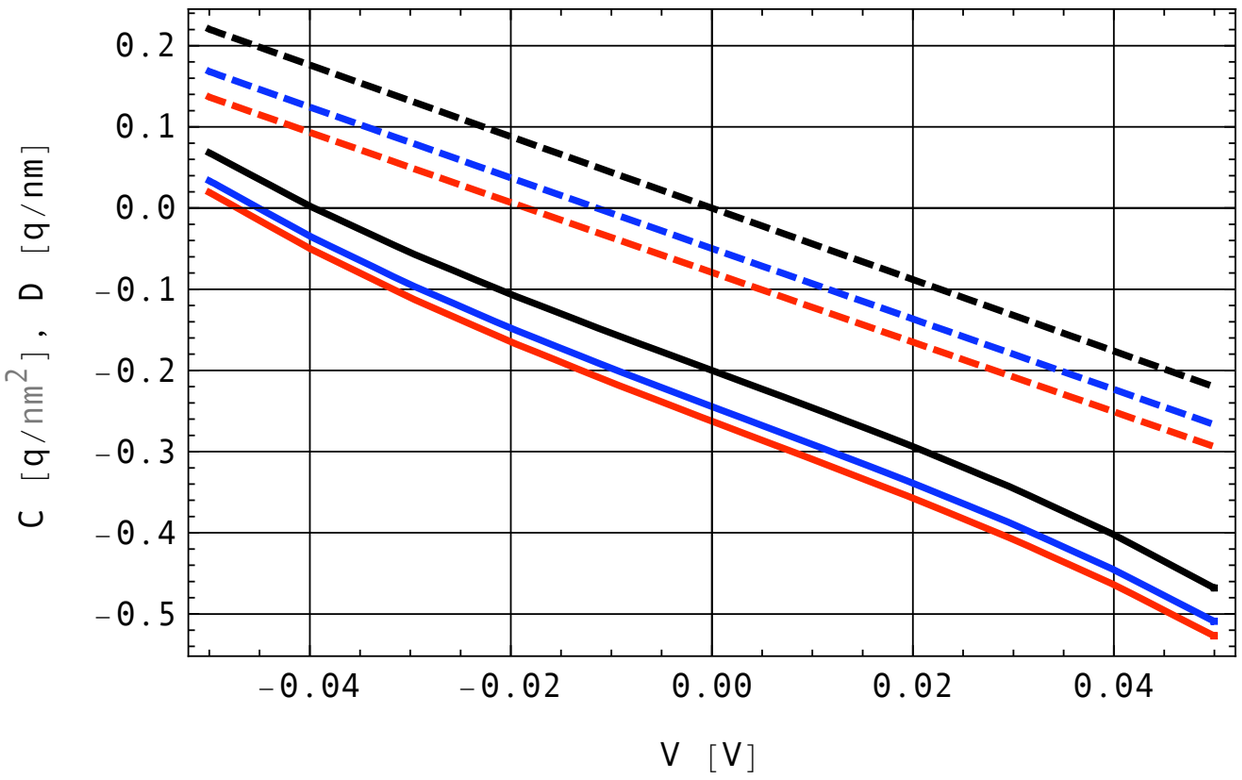

Boundary layer	Specific conductance	
No molecules	2.29E–6 S/m	0%
ssDNA	2.58E–6 S/m	+12.7%
dsDNA	2.91E–6 S/m	+12.8%

universität wien

FTIR ATR spectroscopy can measure molecule density and orientation

Fourier-transformed infrared (FTIR) attenuated total reflection (ATR) spectroscopy provides in-situ quantitative information about chemical bonds at a Si or Ge wafer and also about their orientations.

Collaboration with Dieter Baurecht's group (U. of Vienna).

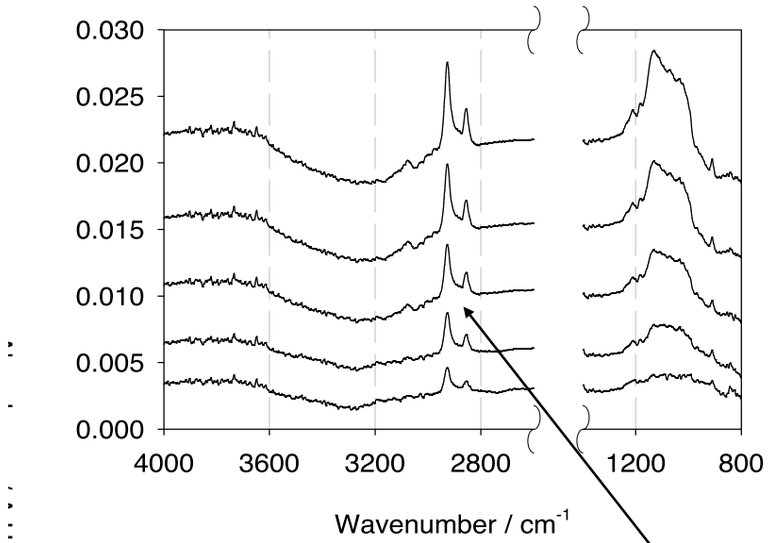

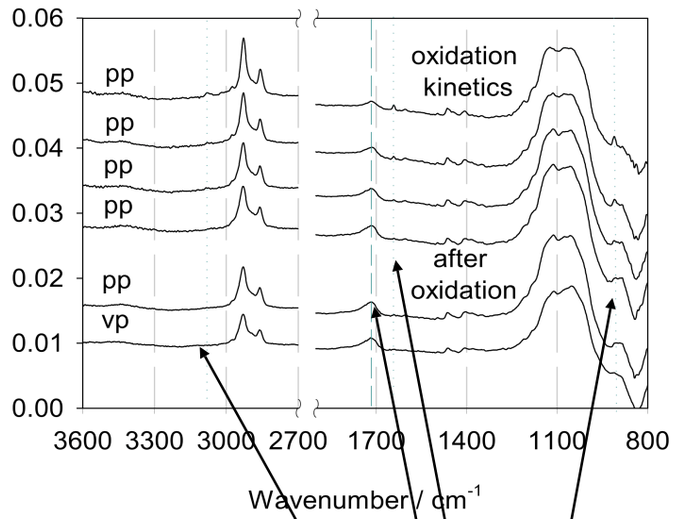

decrease of C=C

increase of C=O

increase of CH_2

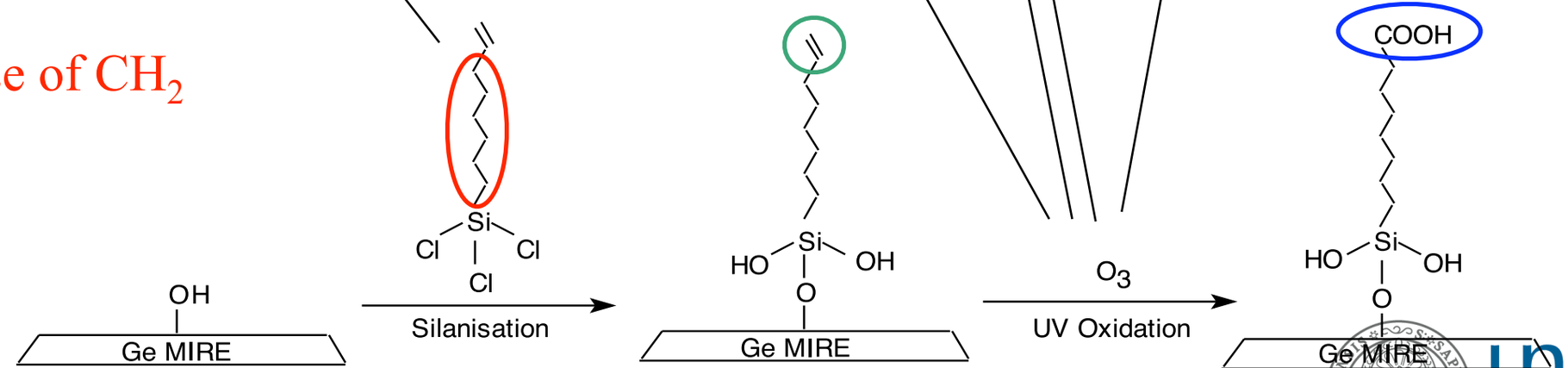

universität wien

3D simulations of nanowire sensors on a substrate

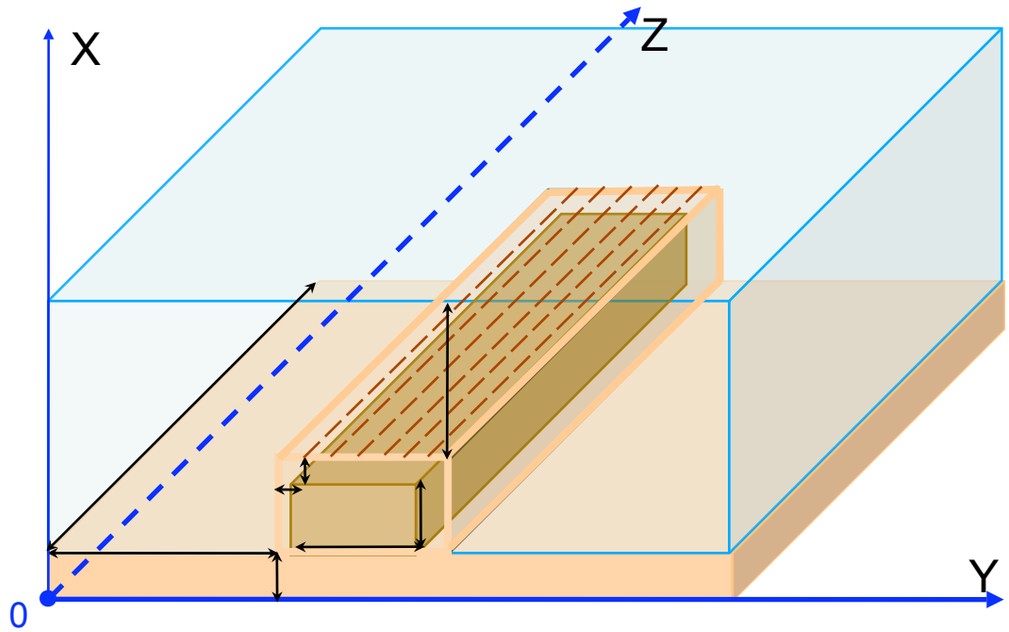

One of the leading experimental groups applies large back-gate voltages to their sensors.

This motivates 3D simulations including our interface conditions.

The efficient implementation of the interface (jump) conditions for the Poisson-Boltzmann equation is not trivial.

Solution: we use an equidistant grid and introduce new equations to identify certain points. This yields the usual band structure.

universität wien

Noise and fluctuations

Noise and fluctuations are important in sensors, especially at the nanoscale (Brownian motion, detection limit etc.).

We consider electrostatic fluctuations due to different charge distributions in a boundary layer at the sensor surface.

The basic model equation is the stochastic Poisson-Boltzmann equation for arbitrary Fermi levels:

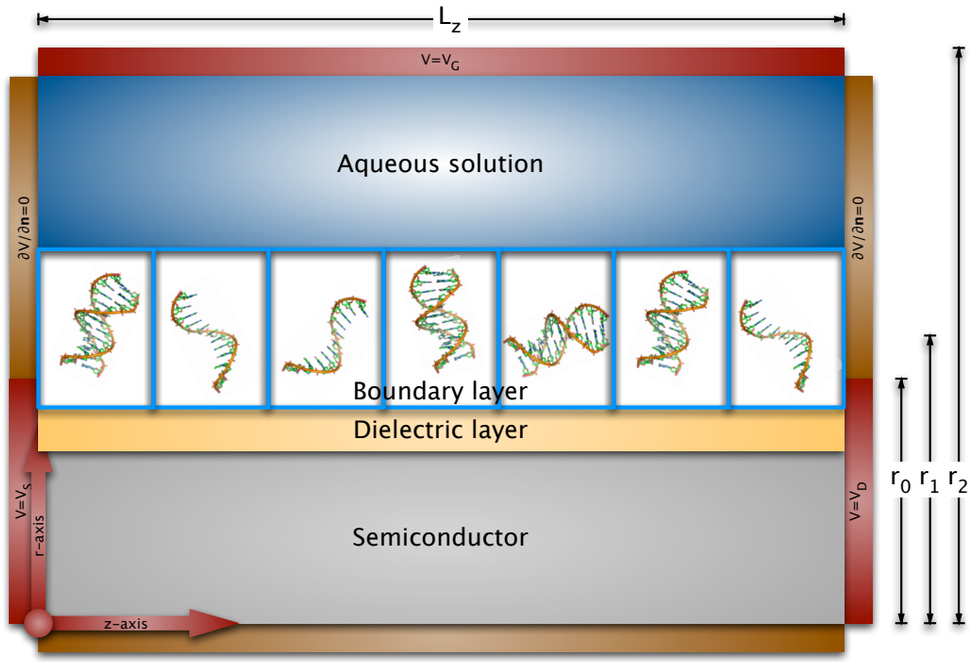

$$
\begin{aligned}
L\phi(x,\omega) &:= -\nabla\cdot\big(A(x,\omega)\nabla\phi(x,\omega)\big)+\gamma(x)\phi(x,\omega),\\
\rho(x,\omega) &:= \rho_f(x,\omega)+\alpha(x),\\
\alpha(x) &:= 2c(x)q\sinh\frac{q(\phi_F-\phi_0)}{k_BT}+\frac{2c(x)q^2\phi_0}{k_BT}\cosh\frac{q(\phi_F-\phi_0)}{k_BT},\\
\gamma(x) &:= \frac{2c(x)q^2}{k_BT}\cosh\frac{q(\phi_F-\phi_0)}{k_BT},\\
L\phi(x,\omega) &= \rho(x,\omega)
\end{aligned}
$$

universität wien

The scaling law for the (co-)variance

We have found a scaling law and an equation for the (co-)variance.

Let ε be the ratio of the size of a cell to the whole domain. We consider a 3-D model with a 2-D boundary layer. Then this scaling law holds:

Scaling law: The covariance scales like ε^4 as $\varepsilon \to 0$.

This is good news for nanoscale sensors!

universität wien

Numerical results for the expectation and variance

The probabilities of the different charge distributions are calculated from their electrostatic free energy.

Then the orientation i with energy E_i is assigned the probability

$p_i := \exp(-E_i / kT) / \Sigma_i \exp(-E_i / kT)$.

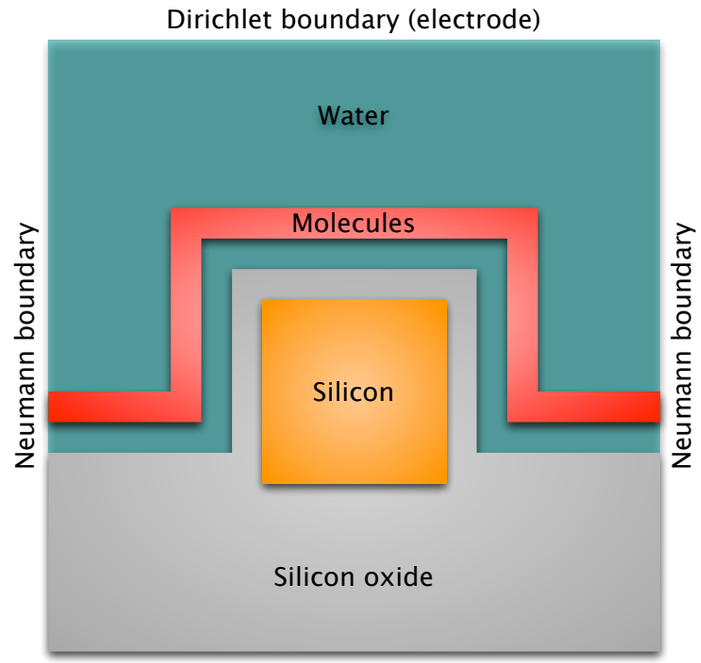

Expectation

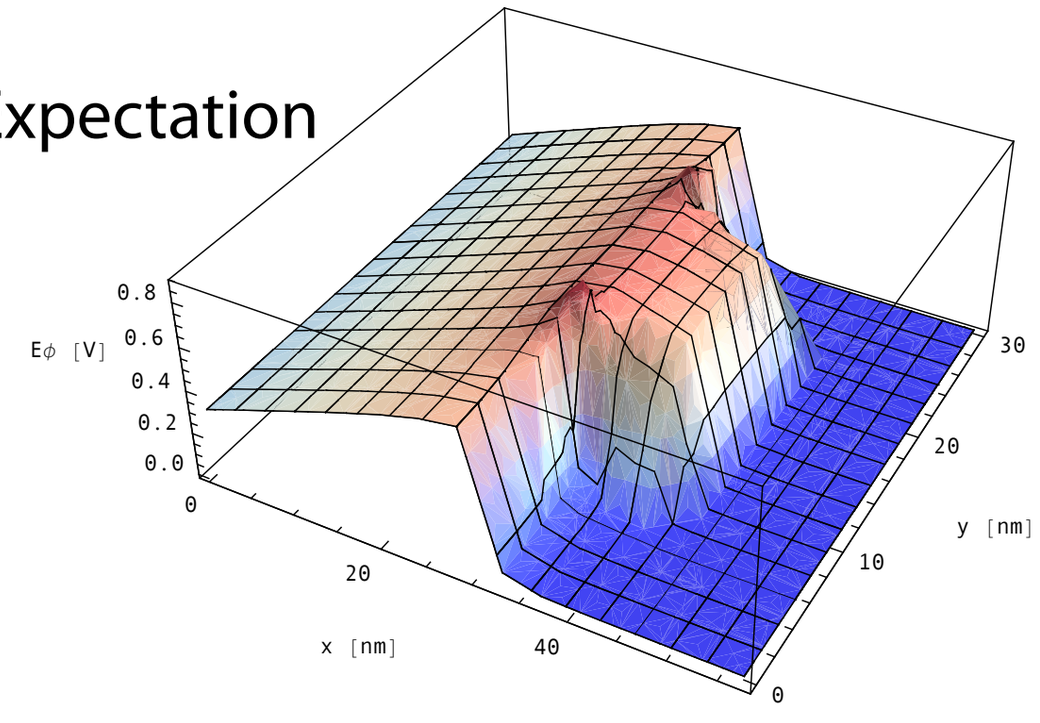

Standard deviation

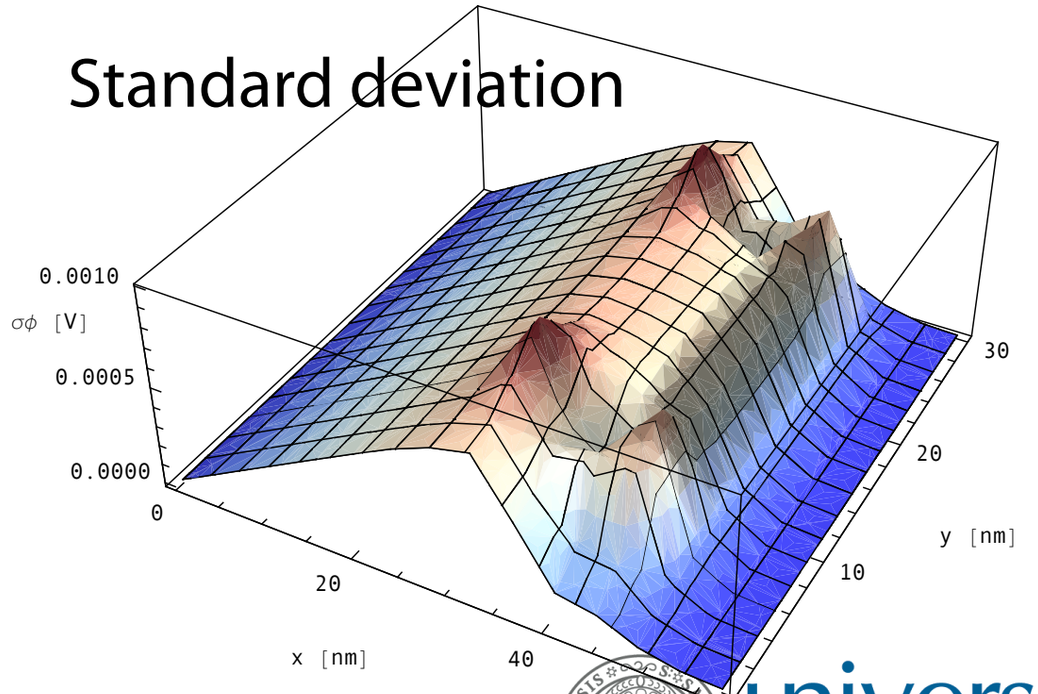

universität wien

Noise in the current

Probe spacing [nm]	Molecules	Current [A]	Change [% of I(Eφ)]
5 nm	50% PNA & 50% ssDNA	$I(E\varphi-\sigma\varphi) = -2.498\cdot10^{-8}$ A $I(E\varphi) = -3.412\cdot10^{-8}$ A $I(E\varphi+\sigma\varphi) = -4.659\cdot10^{-8}$ A	−26.78 0.0 +36.58
5 nm	100% ssDNA	$I(E\varphi-\sigma\varphi) = -2.311\cdot10^{-8}$ A $I(E\varphi) = -2.512\cdot10^{-8}$ A $I(E\varphi+\sigma\varphi) = -2.731\cdot10^{-8}$ A	−8.020 0.0 +8.719
5 nm	50% ssDNA & 50% dsDNA	$I(E\varphi-\sigma\varphi) = -1.275\cdot10^{-8}$ A $I(E\varphi) = -1.803\cdot10^{-8}$ A $I(E\varphi+\sigma\varphi) = -2.549\cdot10^{-8}$ A	−29.27 0.0 +41.38
5 nm	100% dsDNA	$I(E\varphi-\sigma\varphi) = -1.156\cdot10^{-8}$ A $I(E\varphi) = -1.294\cdot10^{-8}$ A $I(E\varphi+\sigma\varphi) = -1.449\cdot10^{-8}$ A	−10.67 0.0 +11.95
10 nm	100% ssDNA	$I(E\varphi-\sigma\varphi) = -3.893\cdot10^{-8}$ A $I(E\varphi) = -3.976\cdot10^{-8}$ A $I(E\varphi+\sigma\varphi) = -4.060\cdot10^{-8}$ A	−2.068 0.0 +2.112
10 nm	100% dsDNA	$I(E\varphi-\sigma\varphi) = -3.274\cdot10^{-8}$ A $I(E\varphi) = -3.368\cdot10^{-8}$ A $I(E\varphi+\sigma\varphi) = -3.464\cdot10^{-8}$ A	−2.782 0.0 +2.862

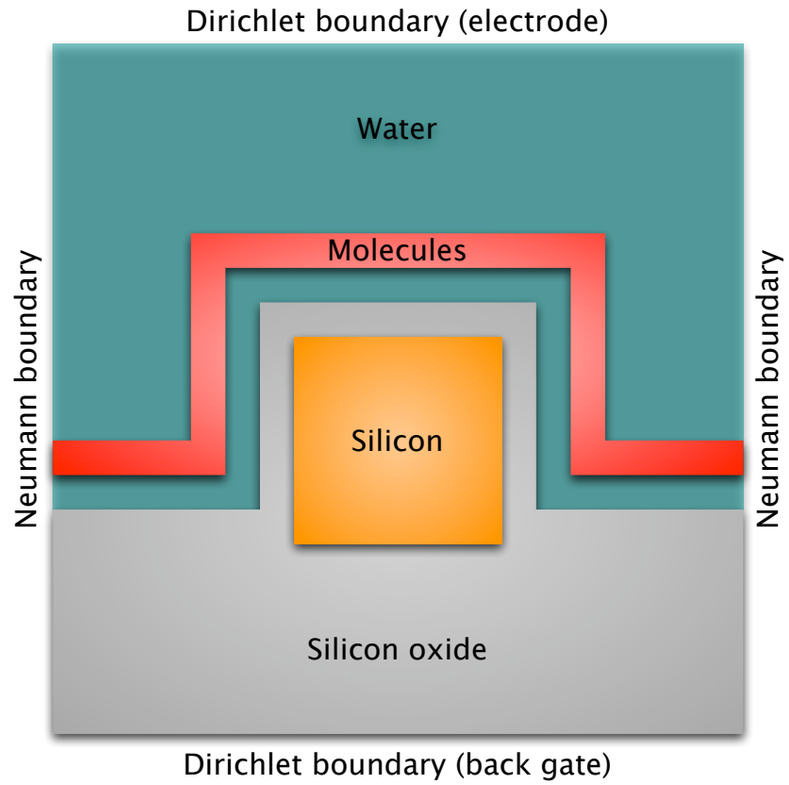

universität wien

How to overcome the screening-induced performance limits of field-effect biosensors

The performance of field-effect sensors is limited by the **screening** of the partial charges of the biomolecules by the (counter-)ions in the liquid.

How can we increase the Debye length?

New idea:
what happens if we add an **electro-diffusion current**?

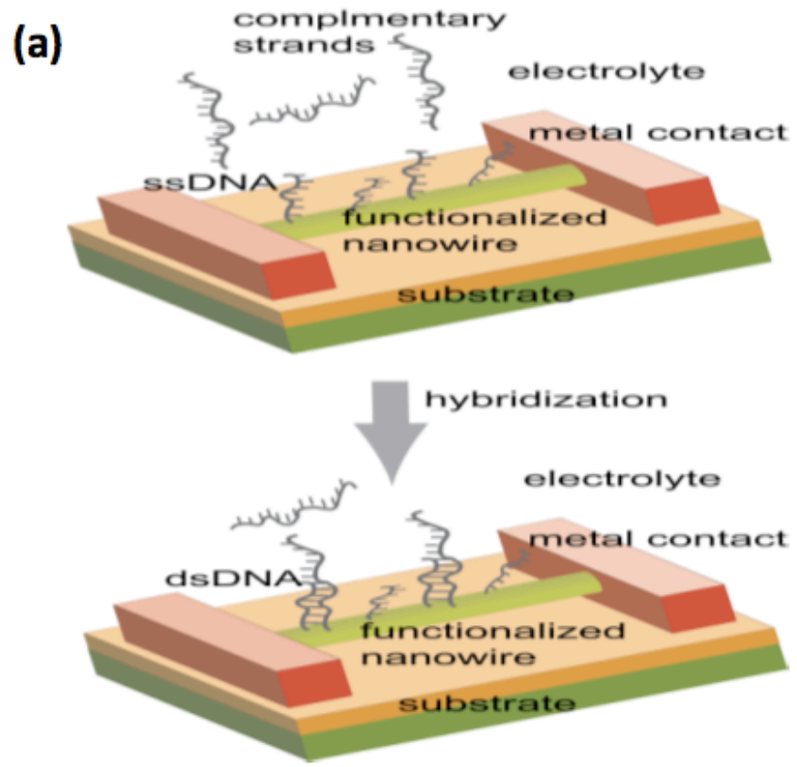

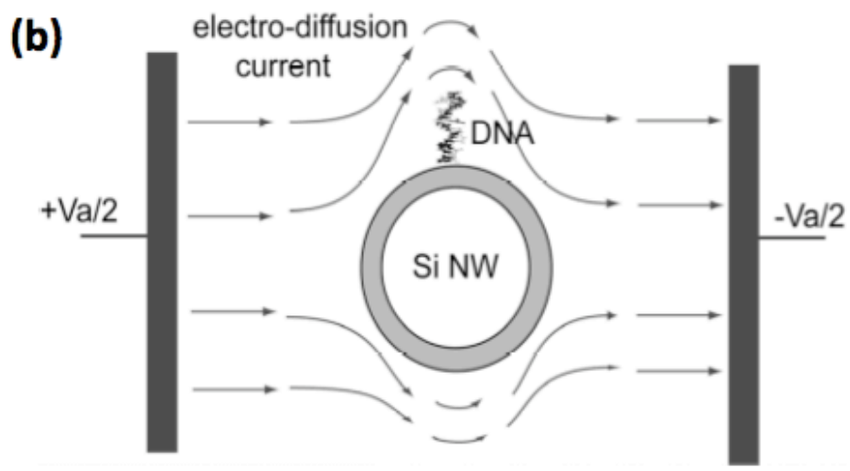

Liu, Lilja, Heitzinger, Dutton. International Electron Devices Meeting (IEDM), San Francisco, CA, December 2008.

universität wien

How to reduce screening: the potential (2-D)

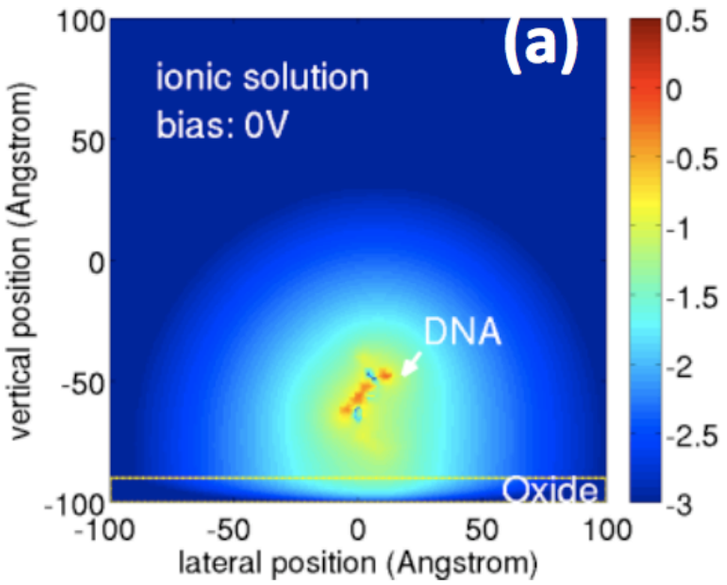

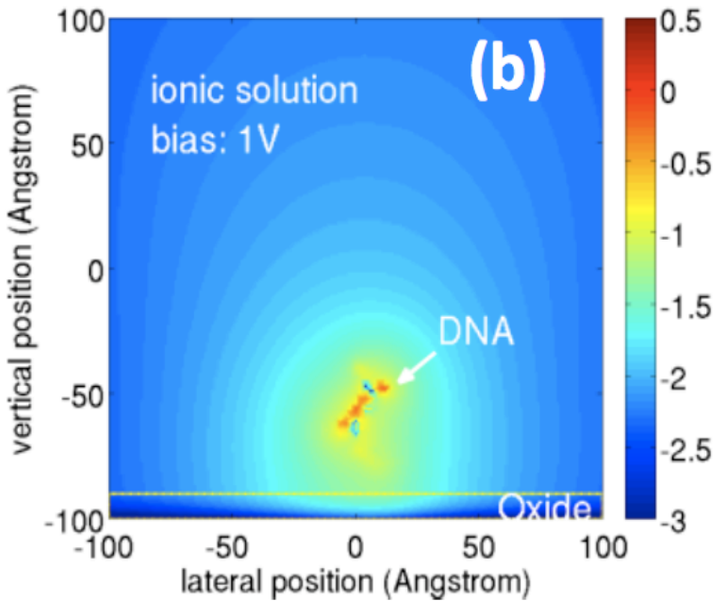

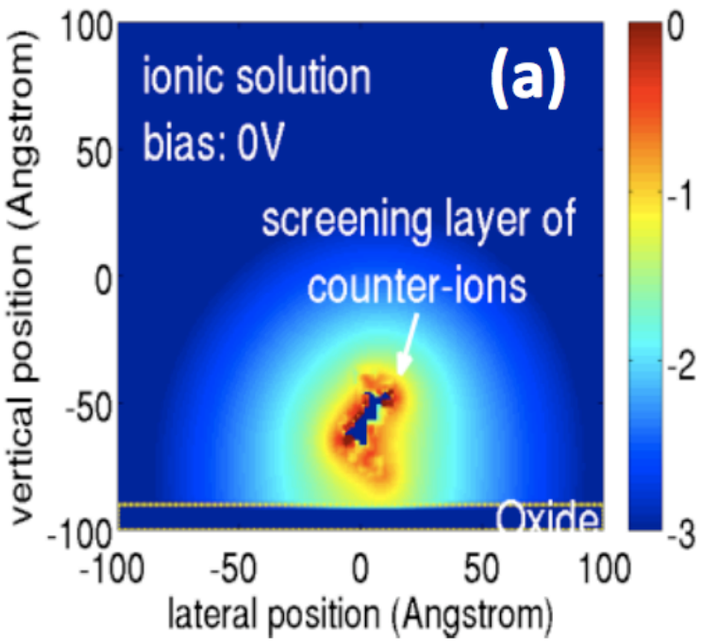

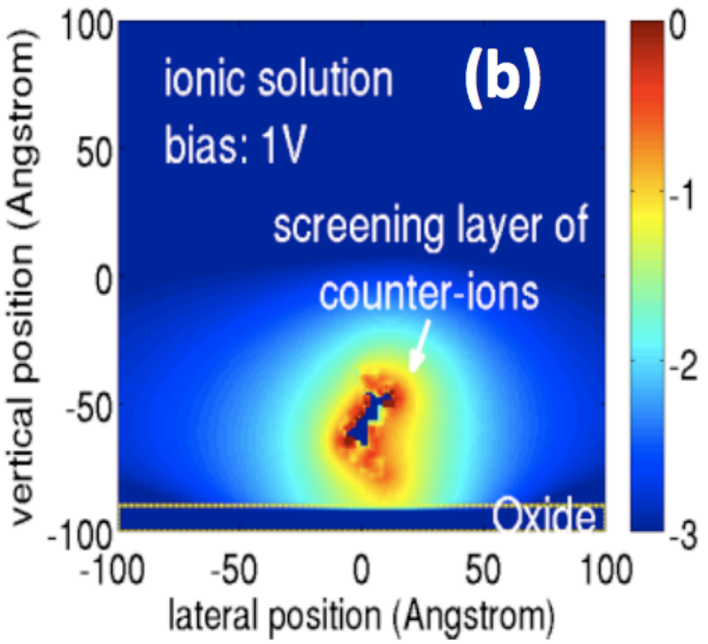

Logarithmic magnitude of the **simulated potential change** (top) and of the **simulated cation density change** (bottom) at a vertical cut-plane of the structure for (a) 0V and (b) 1V electrolyte bias.

The potential change is obtained as the potential difference between the cases with or without a 12 base-pair DNA at the center.

universität wien

How to reduce screening: the conductance (3-D)

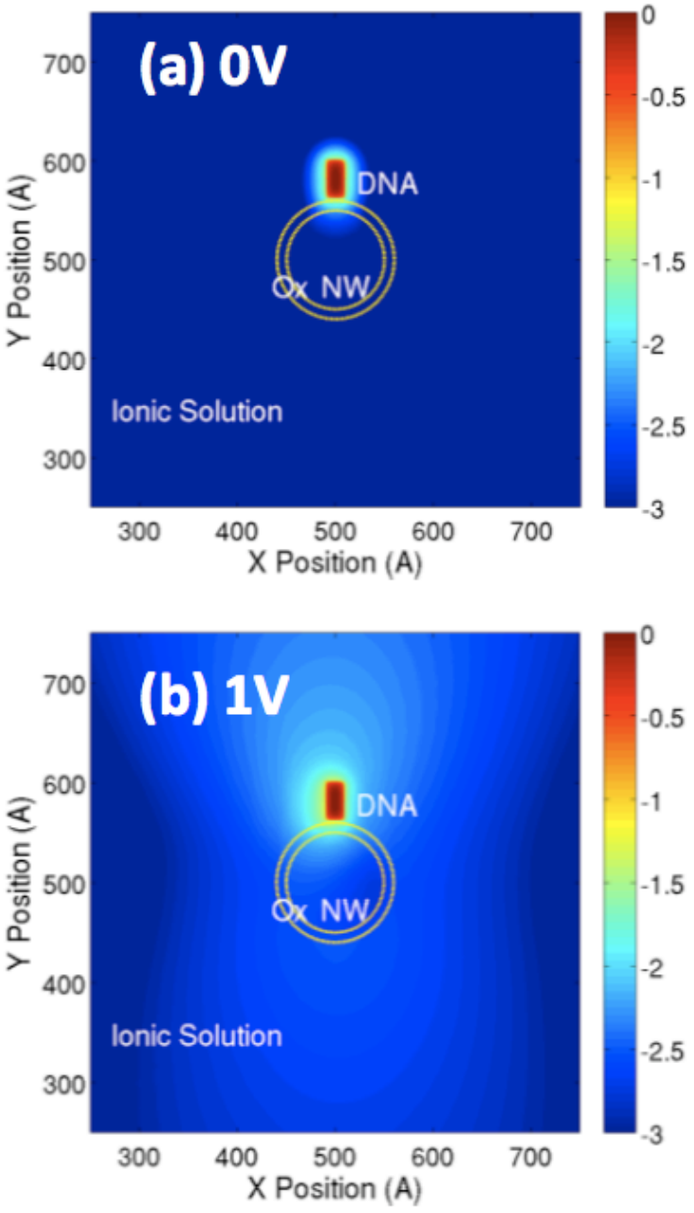

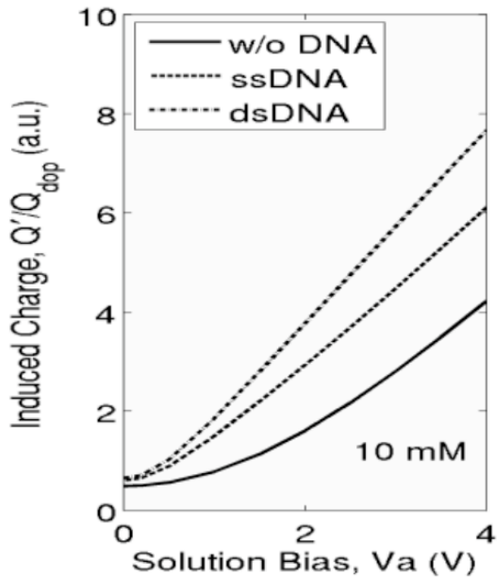

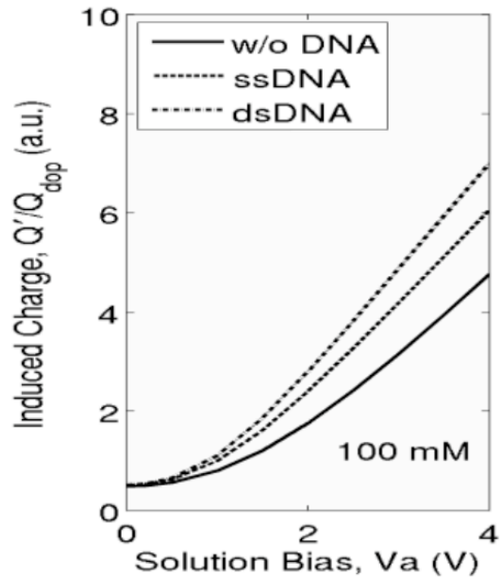

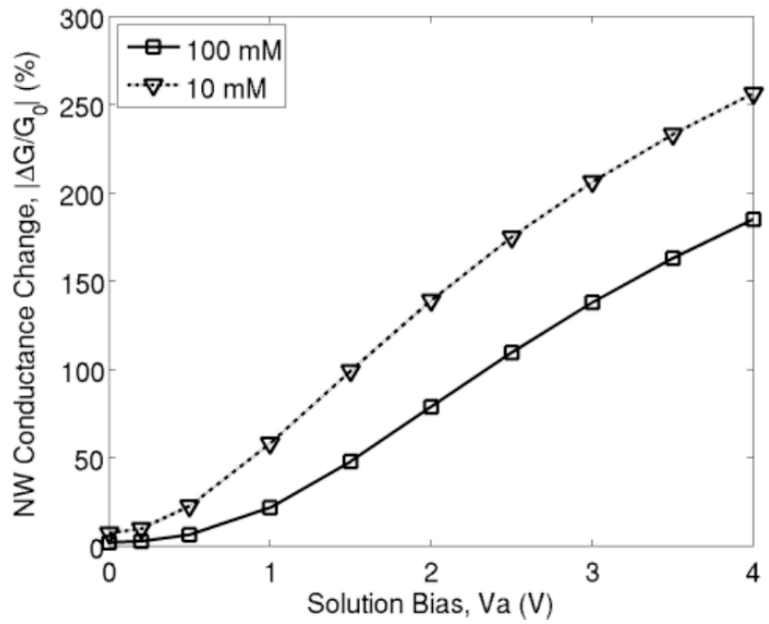

Left: logarithmic magnitude for simulated **potential change** at a lateral cut-plane for (a) 0V and (b) 1V.

Top left: **charge induced** in silicon nanowire (normalized by doping) as a function of electrolyte biases (10mM and 100mM).

Top right: (normalized) silicon nanowire **conductance** change between ssDNA and dsDNA cases as a function of electrolyte biases. At 1V, **enhancement factors** of **11x** (at 100mM) and **8x** (at 10mM) are seen.

universität wien

Conclusion

The **problem**:

- **Field-effect** nano-biosensors are a technology with many biomedical applications. How they work has not been understood at a **quantitative** level.
- The goal is to provide models to understand the physics of the sensors and to enable their **rational design**.

New algorithms for physics-based modeling:

- We have solved the multi-scale problem by deriving **homogenized interface conditions** for arbitrary geometries.
- We developed a constant-voltage ensemble **MC algorithm** that includes biomolecules.
- Our models enable the **self-consistent** simulation of all the charges in the devices. This makes **predictive** investigations possible.
- There are **no fitting parameters** in the models.
- Good **agreement with experiments** has been found.
- A numerical study has shown how **screening-induced performance limits** can be overcome.

universität wien

	Prof. Norbert **Mauser** *Department of Mathematics & Wolfgang Pauli Institute,* *University of Vienna*
	Prof. Christoph **Überhuber** *Institute for Analysis and Scientific Computing,* *TU Vienna*
	Mag. Alena **Bulyha** (doctorate student) *Department of Mathematics & Wolfgang Pauli Institute,* *University of Vienna*
	Stefan **Baumgartner** (master's student) *Department of Mathematics & Wolfgang Pauli Institute,* *University of Vienna*
	Prof. Dieter **Baurecht** *Institute for Biophysical Chemistry,* *University of Vienna*
	Prof. Heidrun **Karlic** *Institute for Leukemia Research and Hematology,* *Ludwig Boltzmann Society, Vienna*
	Dr. Franz **Varga** *Institute for Osteology,* *Ludwig Boltzmann Society, Vienna*
	Mag. Manuel **Punzet** (doctorate student) *Institute for Biophysical Chemistry,* *University of Vienna*

universität wien

	Prof. Christian **Ringhofer** *Department of Mathematics and Statistics, Arizona State University, &* *Wolfgang Pauli Institute, Vienna*
	Prof. Robert W. **Dutton** *Department of Electrical Engineering & Center for Integrated Systems,* *Stanford University*
	Dr. Yang **Liu** *Center for Integrated Systems,* *Stanford University*

ÖAW	ÖAW (Austrian Academy of Sciences) jubilee-fund project *Multi-Scale Modeling and Simulation of Field-Effect Nano-Biosensors*
FWF	FWF (Austrian Science Fund) project *Mathematical Models and Characterization of BioFETs*

Publications are available at http://Clemens.Heitzinger.name/

universität wien